Spontaneous symmetry breaking and response functions

A. Beraudo, A. De Pace, M. Martini and A. Molinari

Dipartimento di Fisica Teorica dell'Università di Torino and
Istituto Nazionale di Fisica Nucleare, Sezione di Torino,
via P.Giuria 1, I-10125 Torino, Italy

Abstract

We study the quantum phase transition occurring in an infinite homogeneous system of spin 1/2 fermions in a non-relativistic context. As an example we consider neutrons interacting through a simple spin-spin Heisenberg force. The two critical values of the coupling strength — signaling the onset into the system of a finite magnetization and of the total magnetization, respectively — are found and their dependence upon the range of the interaction is explored. The spin response function of the system in the region where the spin-rotational symmetry is spontaneously broken is also studied. For a ferromagnetic interaction the spin response along the direction of the spontaneous magnetization occurs in the particle-hole continuum and displays, for not too large momentum transfers, two distinct peaks. The response along the direction orthogonal to the spontaneous magnetization displays instead, beyond a softened and depleted particle-hole continuum, a collective mode to be identified with a Goldstone boson of type II. Notably, the random phase approximation on a Hartree-Fock basis accounts for it, in particular for its quadratic — close to the origin — dispersion relation. It is shown that the Goldstone boson contributes to the saturation of the energy-weighted sum rule for $\approx 25\%$ when the system becomes fully magnetized (that is in correspondence of the upper critical value of the interaction strength) and continues to grow as the interaction strength increases.

Key words: spontaneous symmetry breaking, response functions, random phase approximation
PACS: 21.60.Jz, 26.60.+c, 75.25.+z, 11.30.Qc

1 Introduction

As emphasized by Iachello [1], atomic nuclei offer an exciting ground to explore phase transitions occurring at different temperatures T. Indeed, for these sys-

tems at $T = 0$ a phase transition is signaled by the change they undergo from spherical to ellipsoidal shapes; at $T \approx 20$ MeV evidence exists for a liquid-gas transition and, finally, at $T \approx 200$ MeV the deconfinement of the hadronic (nuclear) matter is conjectured to take place.

As it is well-known, at $T = 0$ the phase transitions are referred to as *quantum phase transitions*. In fact, they occur in correspondence to special (critical) values of a coupling constant, viewed as a continuous variable, entering into the nuclear Hamiltonian: thus, they are driven, rather than by thermal fluctuations, as it is the case at finite T, by quantum fluctuations.

In connection with quantum fluctuations, besides atomic nuclei, also neutron stars are systems worth to be explored. Indeed, the strong magnetic field present in these systems might be generated by a strong ferromagnetic core in the stellar interior. Although a lot of effort has been devoted to this issue (see Refs. [2,3,4,5,6] for some recent work), no firm conclusions have been reached at present.

In this paper we do not attempt a realistic calculation of the spin polarization of a neutron star, but rather we address general aspects of a quantum phase transition in an infinite homogeneous system of interacting neutrons, viewing the strength V_1 of a spin-spin ferromagnetic neutron-neutron force (admittedly schematic with no pretense of being realistic) as a control parameter. In Ref. [7] we have indeed found that a critical value of the control parameter, namely $V_{1c}^{\rm lower}$, exists such that, for $V_1 \geq V_{1c}^{\rm lower}$, an incipient ferromagnetism sets in into the system. We have computed $V_{1c}^{\rm lower}$, following two different paths:

- Random Phase Approximation (RPA) on a Hartree-Fock (HF) basis (RPA-HF),
- anomalous single-particle propagator formalism,

the latter only in the case of a zero-range force, finding that they lead to identical results.

As it is well-known, the onset of the ferromagnetic phase into an infinite, homogeneous system is signaled, on the one hand, by the divergence of the system spin response function at vanishing frequency in the limit ($\omega = 0, \vec{q} \rightarrow 0$), corresponding, in coordinate space, to a very large spin-spin correlation length at the critical point. On the other hand, in the broken phase the order parameter $< \widehat{M} >$ ($\widehat{M}$ being the system's magnetization operator) acquires a finite expectation value: in Ref. [7] we obtained the latter through the Stoner equation [8]. Equivalently one says that a vanishing (or a finite) value of $< \widehat{M} >$ corresponds to a symmetric (or to a broken) vacuum, respectively.

A second critical value $V_{1c}^{\rm upper}$ of the control parameter, associated to the system's full magnetization or to a completely broken vacuum, exists and was

found in Ref. [7] in the anomalous propagator framework only for the case of a zero-range interaction. In the present work we first explore the impact of the finite range of the force, embedded in a parameter λ, on $V_{1c}^{\rm upper}$. This task was already carried out in Ref. [7] for $V_{1c}^{\rm lower}$, which was computed as a function of λ/k_F, k_F being the Fermi momentum of the system, in the RPA-HF framework. Here we employ the anomalous propagator formalism which allows not only to test the previous RPA-HF results for $V_{1c}^{\rm lower}(\lambda/k_F)$, but also to get the range dependence of the upper critical value.

A second issue addressed in this work relates to the nature of the collective modes of the system *in the broken vacuum*. In this connection one should distinguish between collective modes in the (longitudinal) z-direction (assumed to coincide with the one along which the system's spontaneous magnetization occurs) and in the direction orthogonal to z (transverse). In the latter case the collective excitations truly represents the Goldstone modes of the system: these inevitably occur in presence of a spontaneous breaking of a continuous symmetry (in the present case the spin-rotational one). We shall later address the issue of the number of these modes: here it suffices to say that in the present case just one Goldstone mode exists.

We compute the collective modes of the system in the RPA-HF framework, using again, for the sake of simplicity, a zero-range ferromagnetic force and determining as a preliminary the region in the (ω, q) plane where the response of the system occurs: this turns out to be different for the modes developing in the z-direction and for those expanding in the plane orthogonal to z.

In the former the region results from the interplay of four parabolas, characterized by the Fermi momenta k_F^+ and k_F^-, for spin up and spin down particles, respectively, which identify the broken vacuum. The values of k_F^+ and k_F^- are set by the strength of the interaction V_1. The four parabolas eventually coalesce into two when the system becomes fully magnetized. In these kinematical domains the response function to a longitudinal probe displays a collective behavior, however embedded in the particle-hole continuum and hence damped. Specifically, when the system is partially magnetized, for not too large values of q — namely where the Pauli principle is active — the response displays two maxima, one of which is strongly softened and enhanced with respect to the free case, whereas the other is pushed up close to the upper boundary of the response, where it almost coincides with the peak already displayed by the free response: this situation is reminiscent of the splitting of the giant dipole resonance in deformed nuclei [9], although the physical interpretation of the upper peak is different in the two cases (see later). For larger q — where the Pauli principle is no longer felt — the two maxima merge into one, still somewhat softened with respect to the free case, if q, while large, is not too large.

Remarkably, for a fully magnetized system — that is for a completely broken vacuum — no collective mode in the z-direction turns out to be possible: an occurrence, however, strictly valid only for a zero-range interaction.

Turning to the transverse collective modes, when the vacuum is broken by a ferromagnetic spin-spin interaction a region free of single-particle response opens up in the corner of the (ω, q) plane: here is where the Goldstone boson lives. Actually the latter, as we shall see, displays — in the combined RPA and HF framework and for not too large momenta — a parabolic (rather than linear) dispersion relation: hence, according to the general theory of the spontaneous symmetry breaking in the non-relativistic regime [10], it turns out to be a Goldstone mode of second kind. It is remarkable that the RPA-HF theory accounts for its existence through a parabolic dispersion relation, which, however, for larger momenta deviates from the parabolic behavior. Indeed, it develops, just before entering into the particle-hole continuum, a maximum that entails the vanishing of the group velocity of the propagating mode.

Much information on the collective motion in a many-body system can be gained already through the moments of the response function, referred to as *sum rules*. In the final part of this work we shall consider the zeroth (S_0) and the first (S_1) moments, commonly called the Coulomb and the energy-weighted sum rules, respectively. Specifically, we shall address the issue of finding out how their value is affected by the amount of symmetry breaking occurring in the vacuum, i. e. in the system's ground state.

The present paper is organized as follows: in Section 2 we deal with the problem of determining the critical values of the control parameters and their dependence upon the range of the interaction. In Section 3 we explore the response of the system in the presence of a spontaneous symmetry breaking. Specifically, we analyze the system's response in the direction (referred to as longitudinal) along which its spontaneous magnetization occurs. In Section 4 we study the system's response orthogonal to the direction of the spontaneous magnetization (referred to as transverse). Here the Goldstone nature of the system collective excited state is thoroughly discussed. Finally, in Section 5, the same issue is addressed in the context of the moments of the system's response functions (the so-called *sum rules*). In the concluding section we summarize our work and shortly discuss the nature of the quantum phase transitions addressed in our research. Also, we shortly discuss their significance for the physics of the atomic nuclei and of the neutron stars.

2 The critical values of the control parameter

We have recalled in the previous Section that unlike the symmetric vacuum, which is specified by just one Fermi momentum k_F, the broken vacuum of our system is characterized by two Fermi momenta k_F^+ and k_F^-: these fix the densities of the particles with spin up and spin down, respectively. The equilibrium condition for our system at zero temperature reads then:

$$\omega^+_{k_F^+} = \omega^-_{k_F^-}, \tag{1}$$

where the single-particle energies

$$\omega^\pm_{\vec{k}} = \omega_{\vec{k}} + \Sigma_{\pm\pm}(k) \tag{2a}$$

$$\omega_{\vec{k}} = \frac{k^2}{2m} \tag{2b}$$

embody the exact Hartree-Fock (HF) self-energy [1] that, while diagonal, is no longer proportional to the unit matrix. Indeed for the interaction (in momentum space)

$$V(k) = V_1 \vec{\sigma}_1 \cdot \vec{\sigma}_2 \frac{\lambda^2}{k^2+\lambda^2} \tag{3}$$

the anomalous HF self-energy turns out to read

$$\begin{aligned}\Sigma_{++}(k_F^+, k_F^-, k) = & \frac{V_1}{6\pi^2}\left[(k_F^+)^3 - (k_F^-)^3\right] \\ & -\frac{V_1\lambda^3}{(2\pi)^2}\left[\frac{k_F^+}{\lambda} - \left(\arctan\frac{k_F^+ - k}{\lambda} + \arctan\frac{k_F^+ + k}{\lambda}\right)\right. \\ & +\frac{1}{4}\left(\frac{(k_F^+)^2}{\lambda k} - \frac{k}{\lambda} + \frac{\lambda}{k}\right)\ln\frac{1+(k_F^+ + k)^2/\lambda^2}{1+(k_F^+ - k)^2/\lambda^2} \\ & +2\left(\frac{k_F^-}{\lambda} - \left(\arctan\frac{k_F^- - k}{\lambda} + \arctan\frac{k_F^- + k}{\lambda}\right)\right. \\ & \left.\left. + \frac{1}{4}\left(\frac{(k_F^-)^2}{\lambda k} - \frac{k}{\lambda} + \frac{\lambda}{k}\right)\ln\frac{1+(k_F^- + k)^2/\lambda^2}{1+(k_F^- - k)^2/\lambda^2}\right)\right]\end{aligned} \tag{4a}$$

for spin up neutrons and

$$\Sigma_{--}(k_F^+, k_F^-, k) = \Sigma_{++}(k_F^-, k_F^+, k) \tag{4b}$$

[1] We remind the reader that, although our interaction is of pure exchange character, an Hartree term arises in the self-energy owing to the broken vacuum (see Ref. [7]).

for the spin down ones.
Then, inserting (4a) and (4b), evaluated at the appropriate value of k, into Eq. (1) one gets the equation

$$\begin{aligned}\frac{1}{2m}\left[(k_F^+)^2-(k_F^-)^2\right] &= \frac{V_1}{3\pi^2}\left[(k_F^+)^3-(k_F^-)^3\right] \\ &+\frac{V_1\lambda^3}{(2\pi)^2}\left[\frac{k_F^- - k_F^+}{\lambda}+\arctan\frac{2k_F^-}{\lambda}-\arctan\frac{2k_F^+}{\lambda}+4\arctan\frac{k_F^+-k_F^-}{\lambda}\right. \\ &+\frac{\lambda}{4k_F^+}\ln\left[1+\left(\frac{2k_F^+}{\lambda}\right)^2\right]-\frac{\lambda}{4k_F^-}\ln\left[1+\left(\frac{2k_F^-}{\lambda}\right)^2\right] \\ &\left.+\frac{(k_F^- - k_F^+)[(k_F^+ + k_F^-)^2+\lambda^2]}{2\lambda k_F^+ k_F^-}\ln\frac{1+(k_F^+ + k_F^-)^2/\lambda^2}{1+(k_F^+ - k_F^-)^2}\right], \end{aligned} \tag{5}$$

which, in the case of a zero-range force, reduces to the simple expression

$$V_1 = -\frac{\pi^2}{m}\frac{(k_F^+)^2-(k_F^-)^2}{(k_F^+)^3-(k_F^-)^3}. \tag{6}$$

Writing in the above the Fermi momenta k_F^+ and k_F^- in terms of the magnetization M of the system according to

$$k_F^\pm = [3\pi^2\rho(1\pm M)]^{1/3} \tag{7}$$

one obtains the Stoner equation for the critical value of the coupling V_1. In the above

$$\rho = \frac{k_F^3}{3\pi^2} = \frac{(k_F^+)^3}{6\pi^2}+\frac{(k_F^-)^3}{6\pi^2} \tag{8}$$

is the density of the system and, of course, $0 \le M \le 1$.

Solving Eq. (5) for $M = 1$, which implies $k_F^+ = 2^{1/3}k_F$, and setting $x = \lambda/k_F$ one gets

$$\begin{aligned}V_{1,c}^{\rm upper} = -\frac{\pi^2}{mk_F}\frac{1}{2^{1/3}}&\left[\frac{2}{3}+\frac{x^2}{x^2+2^{2/3}}+\frac{x^2}{2\ 2^{2/3}}+\frac{x^2}{2^{2/3}}\frac{x^2}{x^2+2^{2/3}}\right. \\ &\left.-x^3\arctan\left(\frac{2^{1/3}}{x}\right)+\frac{x^3}{4}\arctan\left(\frac{2\ 2^{1/3}}{x}\right)-\frac{x^4}{2^3\ 2^{4/3}}\ln\left(1+4\frac{2^{2/3}}{x^2}\right)\right]^{-1}. \end{aligned} \tag{9}$$

This formula, though cumbersome, becomes transparent for a zero range interaction ($x \to \infty$), where it reads

$$\lim_{x\to\infty} V_{1,c}^{\rm upper} = -\frac{\pi^2}{mk_F}\frac{1}{2^{1/3}}, \tag{10}$$

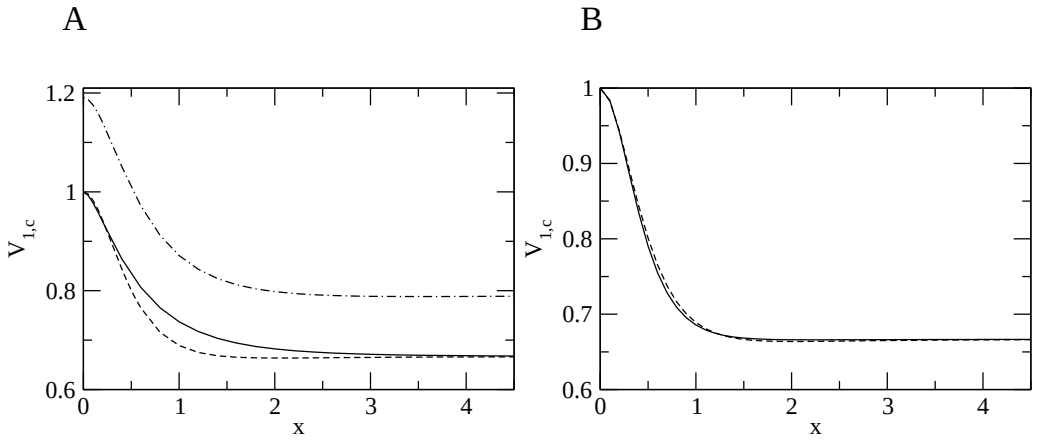

Fig. 1. In panel (A) the behavior of the critical couplings $V_{1,c}^{\rm upper}$ (dot-dashed) and $V_{1,c}^{\rm lower}$ (solid) computed in the anomalous propagator formalism are shown versus $x = \lambda/k_F$; also displayed is $V_{1,c}^{\rm lower}$ in RPA-HF (dashed). In panel (B) one sees $V_{1,c}^{\rm lower}$ in the effective mass approximation both in the anomalous propagator framework (solid) and in RPA-HF (dashed). All curves are in units of $-\pi^2/mk_F$.

a value coinciding with the one found in Ref. [7], while for an infinite range force ($x \to 0$), where it yields

$$\lim_{x\to 0} V_{1,c}^{\rm upper} = -\frac{\pi^2}{mk_F}\frac{1}{2^{1/3}}\frac{3}{2}. \tag{11}$$

The behavior of the absolute value of $V_{1,c}^{\rm upper}$ is shown in Fig. 1 (panel A). Note that the actual strength of the interaction (3) is $V_1\lambda^2$: it would display a monotonically increasing behavior with λ, showing that the larger the range of the force, the smaller the resistance of the medium to become fully magnetized. It is worth reminding that this behavior is shared by the $O(3)$ model [11], which enjoys the same symmetry of ours and represents a generalization of the Ising model [12]. Also remarkable is that for ranges of the force smaller than about $(2k_F)^{-1}$ the critical value of the control parameter becomes essentially insensitive to λ.

In concluding this Section we quote the lower critical value of the coupling V_1 as obtained through the Stoner Equation. For this purpose it merely suffices to solve Eq. (5) setting $< \widehat{M} >= 0$. One gets

$$V_{1,c}^{\rm lower} = -\frac{\pi^2}{mk_F}\left[1 + \frac{x^2}{2}(1+\frac{3}{8}x^2)\ln(1+\frac{4}{x^2}) - \frac{3}{4}x^2\right]^{-1}, \tag{12}$$

which for a zero-range interaction reduces to

$$\lim_{x\to\infty} V_{1,c}^{\rm lower} = -\frac{\pi^2}{mk_F}\cdot\frac{2}{3}, \tag{13}$$

a value coinciding with what found in [7] and for an infinite range force yields

$$\lim_{x\to 0} V_{1,c}^{\rm lower} = -\frac{\pi^2}{mk_F}. \tag{14}$$

Formula (12) is displayed in Fig. 1 (panel A) as a function of x. In the same figure it is also shown the result obtained in Ref. [7] through the solution of the RPA equation in the long wave length, small frequency domain [13]. Notably the two curves differ at intermediate value of x. This outcome relates to the approximation made in Ref. [7], namely of using the effective mass as an approximation to the self-consistent HF solution. Indeed, if we do the same in the present anomalous propagator framework, we find for the neutron self energy

$$\Sigma_{++}^{\rm eff}(k_F^+, k_F^-, k) = A_{++} + B_{++}k^2, \tag{15}$$

with

$$\begin{aligned} A_{++} =& \frac{V_1}{6\pi^2}\left[(k_F^+)^3 - (k_F^-)^3\right] \\ & -\frac{V_1\lambda^3}{(2\pi)^2}\left[\left(\frac{k_F^+}{\lambda} - \arctan\frac{k_F^+}{\lambda}\right) + 2\left(\frac{k_F^-}{\lambda} - \arctan\frac{k_F^-}{\lambda}\right)\right] \qquad (16a) \\ B_{++} =& \frac{V_1\lambda^2}{6\pi^2}\left[\frac{(k_F^+)^3}{((k_F^+)^2+\lambda^2)^2} + 2\frac{(k_F^-)^3}{((k_F^-)^2+\lambda^2)^2}\right] \qquad (16b) \end{aligned}$$

and

$$\Sigma_{--}^{\rm eff}(k_F^+, k_F^-, k) = \Sigma_{++}^{\rm eff}(k_F^-, k_F^+, k). \tag{17}$$

It is gratifying to see in Fig. 1 (panel B) that now, namely in the effective mass approximation, the anomalous propagator framework and the RPA-HF lead to identical results.

3 The system's longitudinal response

Let us assume the system to undergo a spontaneous symmetry breaking acquiring a magnetization along the z-axis. We wish to explore the system's response to a spin-dependent, but not spin-flipping, external probe acting in the z direction, namely described by an operator

$$\widehat{O} = \sum_{\substack{r\beta \\ s\alpha}} < r\beta|\sigma_z|s\alpha > \hat{a}_{r\beta}^\dagger \hat{a}_{s\alpha} = \sum_{s\alpha} \hat{a}_{s\alpha}^\dagger \hat{a}_{s\alpha}(-1)^{1/2-\alpha}. \tag{18}$$

For sake of simplicity we confine ourselves to assume a ferromagnetic ($V_1 < 0$), spin-dependent, zero-range interaction among neutrons, namely

$$V(r) = V_1 \vec{\sigma}_1 \cdot \vec{\sigma}_2 \delta(r), \tag{19}$$

clearly constant in momentum space (see Eq.(3) in $\lambda \to \infty$ limit).

We shall compute the response to the probe (18) in the RPA-HF framework both in a normal and in a broken vacuum. To this end it is first necessary to set up the longitudinal HF anomalous polarization propagator in the broken vacuum $\Pi_{zz}^{\mathrm{HF},b}$. This is easily achieved starting from the anomalous single-particle propagator (the label "b" stands for "broken vacuum")

$$G^{\mathrm{HF},b}(\vec{k},k_0)=\begin{pmatrix} G_{++}^{\mathrm{HF},b}(\vec{k},k_0) & 0 \\ 0 & G_{--}^{\mathrm{HF},b}(\vec{k},k_0)\end{pmatrix}, \tag{20}$$

where

$$G_{++}^{\mathrm{HF,b}}(\vec{k},k_0)=\frac{\theta(k-k_F^+)}{k_0-\omega_{\vec{k}}^+ +i\eta}+\frac{\theta(k_F^+-k)}{k_0-\omega_{\vec{k}}^+ -i\eta} \tag{21a}$$

is the propagator for a spin up neutron and

$$G_{--}^{\mathrm{HF,b}}(\vec{k},k_0)=\frac{\theta(k-k_F^-)}{k_0-\omega_{\vec{k}}^- +i\eta}+\frac{\theta(k_F^--k)}{k_0-\omega_{\vec{k}}^- -i\eta} \tag{21b}$$

is the propagator for a spin down one and

$$\omega_{\vec{k}}^{\pm}=\frac{k^2}{2m}-\frac{V_1 k_F^{\mp 3}}{2\pi^2} \tag{22}$$

are the single-particle energies (2) for a zero-range force. In the following we shall specify the spin indices for G only, dropping all the other ones, and we shall always assume the HF approximation for the single-particle propagator.

One gets then for the HF polarization propagator in the z-direction and in the broken vacuum, setting $K\equiv(k_0,\vec{k})$ and $Q\equiv(\omega,\vec{q})$,

$$\begin{aligned}\Pi_{zz}^{\mathrm{HF},b}(Q)&=-i\int\frac{\mathrm{d}^4K}{(2\pi)^4}[G_{++}(K)G_{++}(K+Q)+G_{--}(K)G_{--}(K+Q)]\\ &=\Pi_{++}^{\mathrm{HF}}(Q)+\Pi_{--}^{\mathrm{HF}}(Q)\end{aligned} \tag{23}$$

being

$$\begin{aligned}\Pi_{++}^{\mathrm{HF}}(Q)=\Pi_{++}^{0}(Q)=&\int\frac{\mathrm{d}\vec{k}}{(2\pi)^3}\theta(|\vec{k}+\vec{q}|-k_F^+)\theta(k_F^+-k)\\ &\times\left[\frac{1}{\omega+\omega_{\vec{k}}-\omega_{\vec{k}+\vec{q}}+i\eta}-\frac{1}{\omega+\omega_{\vec{k}+\vec{q}}-\omega_{\vec{k}}-i\eta}\right]\end{aligned} \tag{24}$$

and

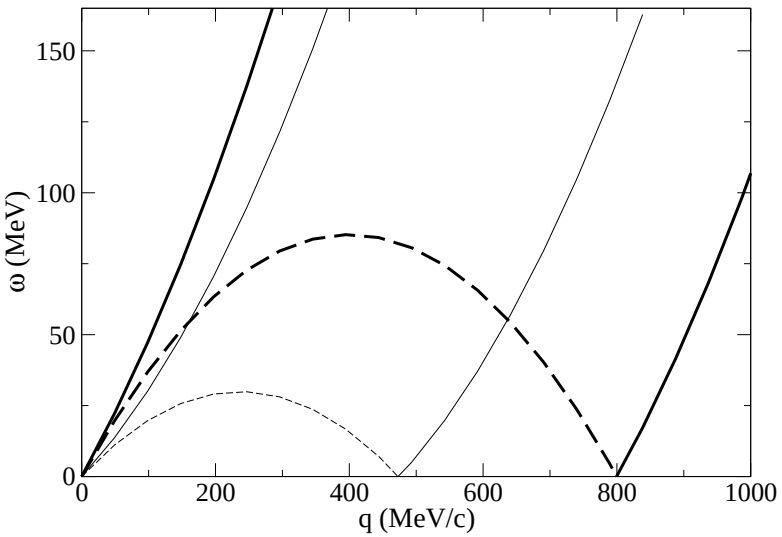

Fig. 2. The response region in a broken vacuum. In the figure $k_F^+ = 400$ MeV/c and $k_F^- = 237$ MeV/c. The heavy (light) line marks the domain where the spin up (down) neutrons respond to an external probe. The dashed lines represent the boundaries of the Pauli blocked regions.

$$\Pi^{\rm HF}_{--}(Q) = \Pi^0_{--}(Q) = \int \frac{{\rm d}\vec{k}}{(2\pi)^3}\theta(|\vec{k}+\vec{q}| - k_F^-)\theta(k_F^- - k) \times \left[\frac{1}{\omega + \omega_{\vec{k}} - \omega_{\vec{k}+\vec{q}} + i\eta} - \frac{1}{\omega + \omega_{\vec{k}+\vec{q}} - \omega_{\vec{k}} - i\eta}\right]. \quad (25)$$

Note that the HF expressions for Π_{++} and Π_{--} are identical to the free ones in the case of a zero-range interaction. Moreover both their real and imaginary part can easily be computed analytically: one clearly obtains the familiar results for a symmetric vacuum [14] with k_F replaced by k_F^+ and k_F^-, respectively.

Eqs. (23), (24) and (25) allow us to display in Fig. 2 the response region of the system, in the frequency ω - momentum q plane, when the vacuum is broken. We see in the figure that the global response region is actually made up by two response domains: one associated with k_F^+, where the particles with spin up respond to the external probe and the other associated with k_F^-, where the particles with spin down respond to the external probe.

Turning to the propagator $\Pi^{\text{RPA-HF},b}_{zz}$ in RPA-HF, it obeys the equation

$$\widehat{\Pi} = \widehat{\Pi}^{\rm HF} + \widehat{\Pi}^{\rm HF}\widehat{V}\widehat{\Pi}, \quad (26)$$

graphically displayed in Fig. 3, where:

$$\widehat{\Pi} = \begin{pmatrix} \Pi_{++} & \Pi_{+-} \\ \Pi_{-+} & \Pi_{--} \end{pmatrix} \quad \widehat{\Pi}^{\rm HF} = \begin{pmatrix} \Pi^{\rm HF}_{++} & 0 \\ 0 & \Pi^{\rm HF}_{--} \end{pmatrix} \quad \text{and} \quad \widehat{V} = \begin{pmatrix} V_d & V_{od} \\ V_{od} & V_d \end{pmatrix}. \quad (27)$$

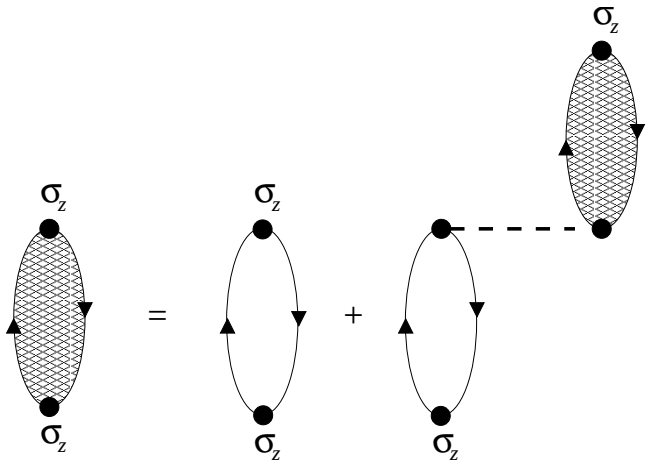

Fig. 3. The Dyson equation for the RPA anomalous polarization propagator.

The solution of Eq. (26) turns out to read (see Appendix A)

$$\Pi_{zz}^{\text{RPA-HF},b} = \frac{\Pi_{++}^{\text{HF}} + \Pi_{--}^{\text{HF}} + 2\Pi_{++}^{\text{HF}}\Pi_{--}^{\text{HF}}(V_{od} - V_d)}{1 - V_d(\Pi_{++}^{\text{HF}} + \Pi_{--}^{\text{HF}}) + \Pi_{++}^{\text{HF}}\Pi_{--}^{\text{HF}}(V_d^2 - V_{od}^2)}. \tag{28}$$

In the above V_d and V_{od} correspond to the diagonal and off-diagonal particle-hole matrix elements of the interaction (19) in spin space: they are given in Appendix A. Noteworthy is that Eq. (28) is formally similar to what one gets in systems containing two species of particles, e.g. nucleons and Δ's (see Ref. [15]).

Equation (28) entails a striking consequence, namely that for a fully broken vacuum (a fully magnetized system, for example in the positive z-direction) no RPA collective mode exists for a zero-range force. Indeed, in this case, since $k_F^- = 0$ then $\Pi_{--}^0 = 0$ and also, as shown in Appendix A, V_d=0. The situation is clearly illustrated in Figs. 4, 5 and 6, where the system's response along the z-axis is shown at $q = 5$, 50 and 500 MeV/c, respectively. Furthermore, in each figure, the evolution of the system's response with the amount of breaking of the vacuum is also displayed. Accordingly, in each figure the responses associated to four pairs of values of k_F^+ and k_F^- are shown: since the density of the system is fixed, these are related by Eq. (8). We further observe that each choice of (k_F^+,k_F^-) corresponds to a value of the strength of the interaction V_1 given by Eq. (6). In panel A of all figures the enhancement and softening of the response in the symmetric vacuum ($k_F^+ = 338.13$ MeV/c), due to the attractive ferromagnetic interaction, is clearly apparent. As one moves towards an increasingly broken vacuum and for not too large momenta one sees the appearance of a second peak in the response at high energy until, for a totally broken vacuum, the collectivity completely disappears in accord with the argument given above and the free response is recovered.

In order to understand the frequency behavior of the response at $q = 5$ and $q = 50$ MeV/c it helps to keep in mind that

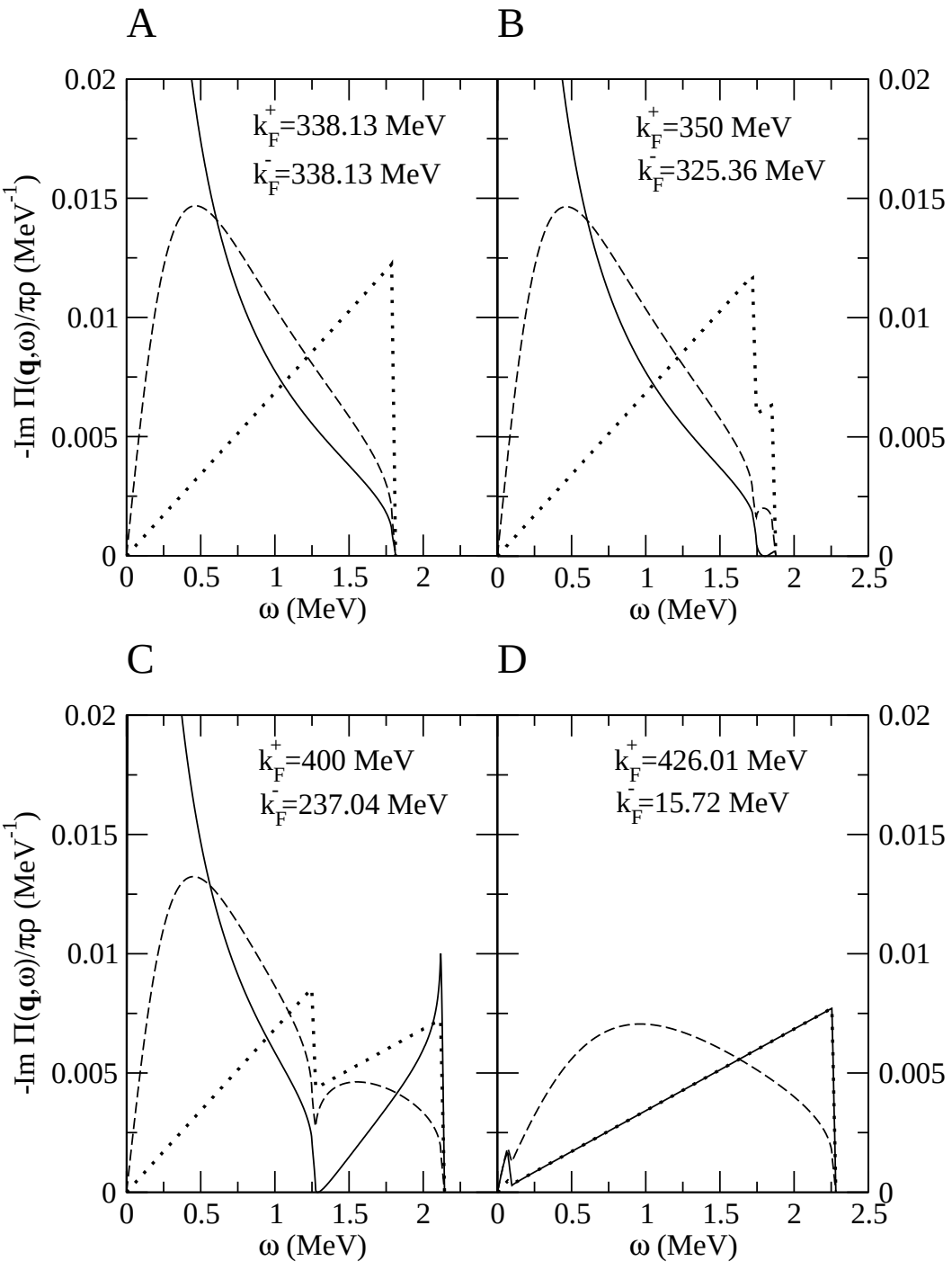

Fig. 4. The response of an infinite neutron's system to a z-aligned probe for $q = 5$ MeV/c. Panel (A) refers to the case of a symmetric vacuum ($k_F = k_F^+ = k_F^-$), panels (B) and (C) to a partially aligned broken vacuum, panel (D) to a totally broken, fully aligned vacuum. Dotted line: HF (free) response, dashed line: ring approximation, solid line: RPA-HF.

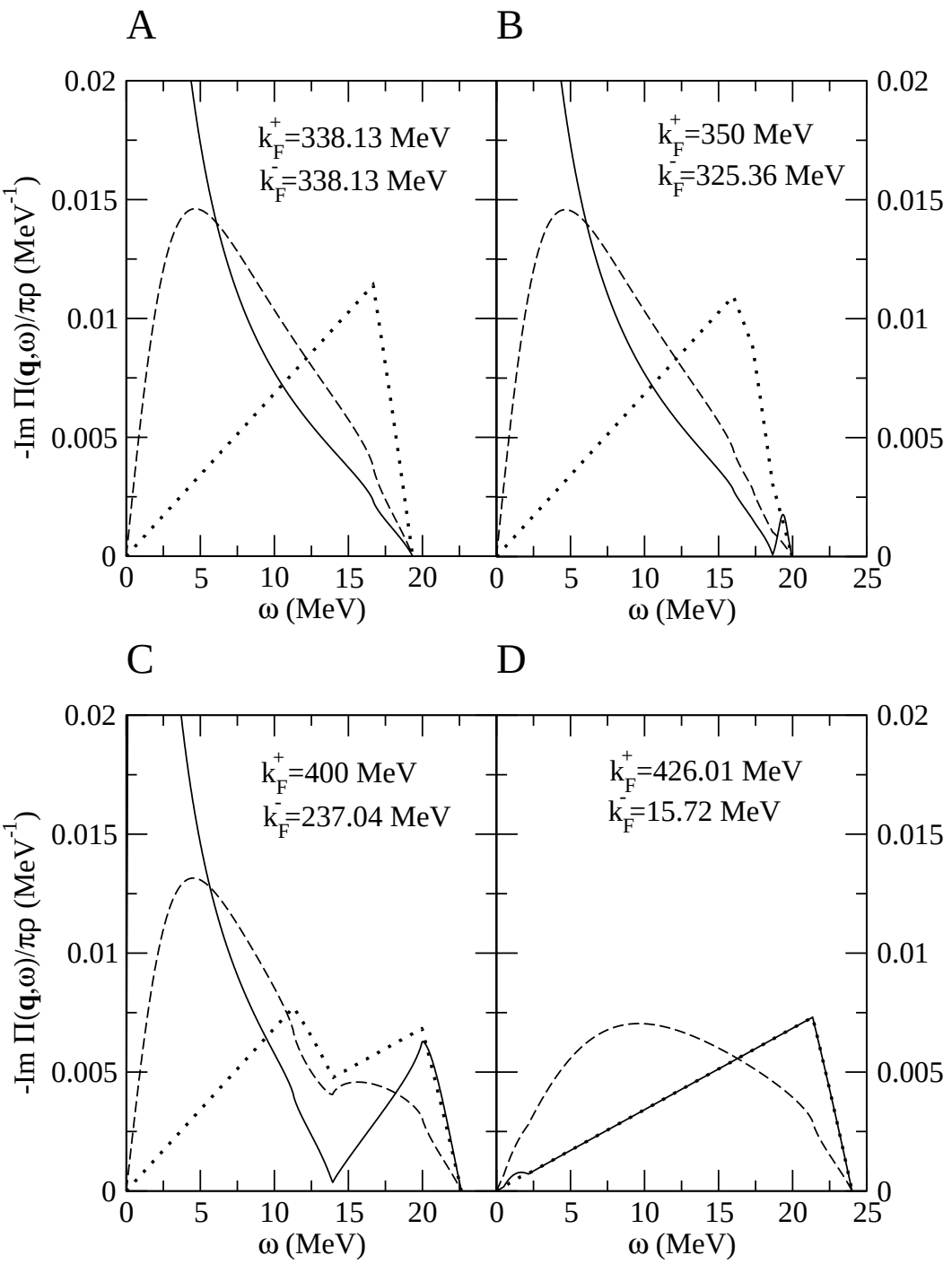

Fig. 5. The same as in Fig. 4 but for $q = 50$ MeV/c.

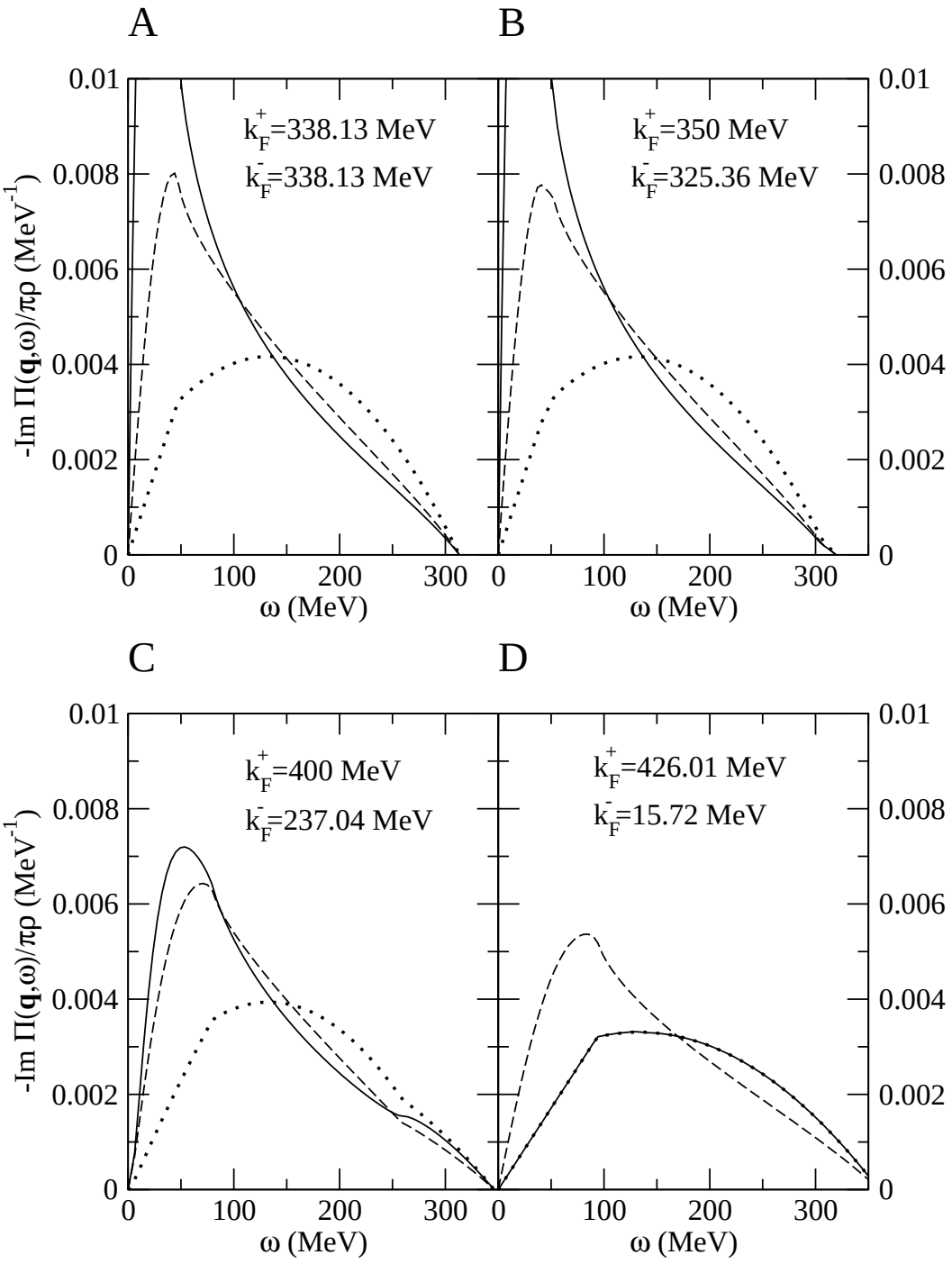

Fig. 6. As in Fig. 4 but for $q = 500$ MeV/c.

a) the HF (free) response in the broken, but not fully so, vacuum already displays two maxima, when the Pauli principle is active (namely for not too large q);
b) the RPA-HF framework conserves the energy-weighted sum rule even when the vacuum is broken (this non trivial result will be further discussed later).

Actually, the RPA-HF expression of the response reads

$$-\frac{1}{\pi\rho}\mathrm{Im}\Pi_{zz}^{\text{RPA-HF,b}} = \frac{N_{\text{RPA-HF}}}{D_{\text{RPA-HF}}}, \tag{29}$$

being

$$N_{\text{RPA-HF}} = -\frac{1}{\pi\rho}\left[\mathrm{Im}(\Pi_{++}^{\text{HF}} + \Pi_{--}^{\text{HF}})(1 - 9V_1^2 u) + 6V_1 v(1 + \frac{3}{2}V_1 \mathrm{Re}(\Pi_{++}^{\text{HF}} + \Pi_{--}^{\text{HF}})\right] \tag{30}$$

and

$$D_{\text{RPA-HF}} = 1 - 18V_1^2 u + (9V_1^2)^2 |\Pi_{++}^{\text{HF}}|^2 |\Pi_{--}^{\text{HF}}|^2, \tag{31}$$

where

$$u = \mathrm{Re}\Pi_{++}^{\text{HF}}\mathrm{Re}\Pi_{--}^{\text{HF}} - \mathrm{Im}\Pi_{++}^{\text{HF}}\mathrm{Im}\Pi_{--}^{\text{HF}} \tag{32}$$

and

$$v = \mathrm{Re}\Pi_{++}^{\text{HF}}\mathrm{Im}\Pi_{--}^{\text{HF}} + \mathrm{Im}\Pi_{++}^{\text{HF}}\mathrm{Re}\Pi_{--}^{\text{HF}}. \tag{33}$$

In the high energy domain where only the spin up neutrons respond to the external probe (namely, where $\mathrm{Im}\Pi_{--}^{\text{HF}} = 0$) the above become

$$N_{\text{RPA-HF}} = -\frac{1}{\pi\rho}\mathrm{Im}\Pi_{++}^{\text{HF}}\left[1 + 6V_1\mathrm{Re}\Pi_{--}^{\text{HF}}(1 + \frac{3}{2}V_1\mathrm{Re}\Pi_{--}^{\text{HF}})\right] \tag{34}$$

and

$$D_{\text{RPA-HF}} = \left(1 - 9V_1^2\mathrm{Re}\Pi_{++}^{\text{HF}}\mathrm{Re}\Pi_{--}^{\text{HF}}\right)^2 + (9V_1^2)^2(\mathrm{Im}\Pi_{++}^{\text{HF}})^2(\mathrm{Re}\Pi_{--}^{\text{HF}})^2, \tag{35}$$

respectively, and since in this regime $\mathrm{Re}\Pi_{--}^{\text{HF}}$ is a rapidly decreasing function of the frequency (see Fig. 7), it follows that the RPA-HF response at large ω approaches the free one and thus the second peak displayed by the latter still shows up.

By contrast, in ring approximation one has the simpler expressions

$$N_{\text{ring}} = -\frac{1}{\pi\rho}\mathrm{Im}(\Pi_{++}^{\text{HF}} + \Pi_{--}^{\text{HF}}) \tag{36}$$

and

$$D_{\text{ring}} = 1 - V_1\mathrm{Re}(\Pi_{++}^{\text{HF}} + \Pi_{--}^{\text{HF}}) + V_1^2\left[\mathrm{Im}(\Pi_{++}^{\text{HF}} + \Pi_{--}^{\text{HF}})\right]^2 \tag{37}$$

which, in the high-frequency regime, become

$$N_{\text{ring}} = -\frac{1}{\pi\rho}\mathrm{Im}\Pi_{++}^{\text{HF}} \tag{38}$$

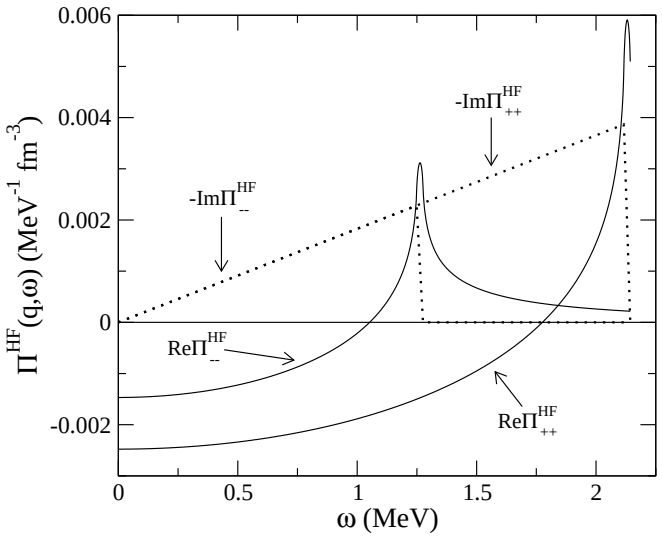

Fig. 7. $\mathrm{Re}\Pi^{\mathrm{HF}}_{\pm\pm}$ (solid) and -$\mathrm{Im}\Pi^{\mathrm{HF}}_{\pm\pm}$ (dot) as a function of ω at $q = 5$ MeV/c. Note that $\mathrm{Re}\Pi^{\mathrm{HF}}_{\pm\pm}$ has a maximum at the upper limit of the corresponding response domain.

and

$$D_{\mathrm{ring}} = 1 - V_1 \mathrm{Re}(\Pi^{\mathrm{HF}}_{++} + \Pi^{\mathrm{HF}}_{--}) + V_1^2 (\mathrm{Im}\Pi^{\mathrm{HF}}_{++})^2. \tag{39}$$

From the last equation it appears that at large ω the ring response is strongly damped.

4 The system's transverse response

In this Section we explore the system's response to a probe aligned in the direction orthogonal to the axis along which the spontaneous magnetization of the system occurs. For definitiveness we choose the probe to act in the x-direction. According to the general theory in a non-relativistic context [10], we expect here Goldstone modes to show up. Their number should not be less than the number of the broken generators of the continuous symmetry, provided that the Goldstone bosons of type II are counted twice. In the case we are presently investigating, the number of the broken generators is provided by the dimensions of the coset $O(3)/O(2)$, where $O(3)$ is the rotation group in three dimensions. This group leaves invariant the Hamiltonian of our system of interacting neutrons, whereas $O(2)$ is the rotation group in two dimensions and represents the surviving symmetry after the spontaneous breaking has occurred. Hence in our case two generators are broken. Accordingly this situation is compatible with the existence either of two Goldstone bosons of type I — characterized by a dispersion relation linear in the momentum — or with the existence of one type II Goldstone boson — which has a dispersion relation quadratic in the momentum.

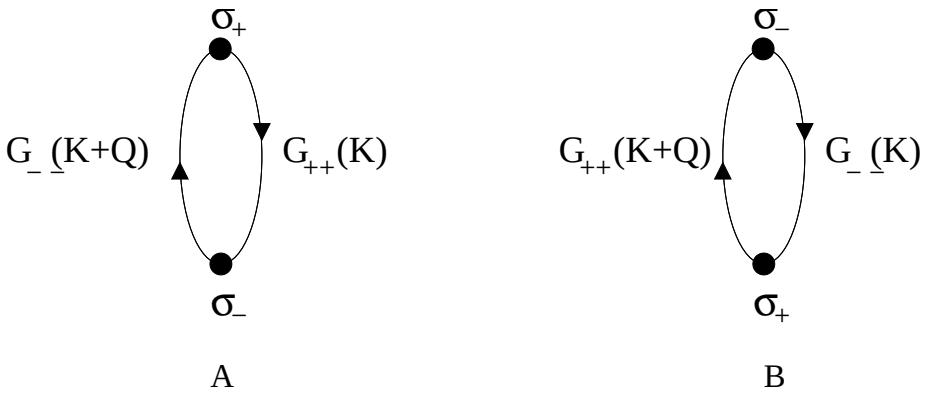

Fig. 8. The diagrams corresponding to $\Pi^{\rm HF}_{-+}(Q)$ (A) and $\Pi^{\rm HF}_{+-}(Q)$ (B).

As we shall see, the latter is actually the occurring case for our system. This is hardly surprising since indeed type II Goldstone bosons are specific of a non-relativistic theory as exemplified by the rotational bands of atomic nuclei, whose energy depends quadratically on the angular momentum (nuclei are finite systems!) [9] and by the pairing additional and removal modes in superconducting nuclei [16], whose energy depends quadratically on the number of pairs. Clearly, in the two above mentioned examples the broken symmetries are the rotational and the global gauge ones, which are spontaneously broken in deformed and superconducting nuclei, respectively. It would be interesting to study a suitable relativistic generalization of our system, since in that case the previously mentioned counting rule for the number of Goldstone bosons no longer holds [17].

In searching for this Goldstone bosons we first ask: where do they live? To answer this question we need to consider the transverse HF polarization propagator

$$\begin{aligned}\Pi^{{\rm HF},b}_{xx/yy}(Q) &= -i\int\frac{{\rm d}^4K}{(2\pi)^4}[G_{++}(K)G_{--}(K+Q)+G_{--}(K)G_{++}(K+Q)]\\ &= \Pi^{\rm HF}_{-+}(Q)+\Pi^{\rm HF}_{+-}(Q),\end{aligned}\tag{40}$$

where we have found it convenient to introduce the quantities $\Pi^{\rm HF}_{-+}$ and $\Pi^{\rm HF}_{+-}$, whose vertices embody the spin operators

$$\sigma_\pm = \frac{1}{2}(\sigma_x \pm i\sigma_y),\tag{41}$$

as shown in Fig. 8. In the HF approximation the expressions for Π_{-+} and Π_{+-} are easily deduced starting from the single particle propagators, already employed in deducing the response to a longitudinal external probe, given in Eqs. (21a) and (21b). One gets:

$$\Pi^{\rm HF}_{-+}(Q) = \int \frac{{\rm d}\vec{k}}{(2\pi)^3} \left[\frac{\theta(|\vec{k}+\vec{q}| - k_F^-)\theta(k_F^+ - k)}{\omega + \omega^+_{\vec{k}} - \omega^-_{\vec{k}+\vec{q}} + i\eta} - \frac{\theta(k_F^- - |\vec{k}+\vec{q}|)\theta(k - k_F^+)}{\omega + \omega^+_{\vec{k}} - \omega^-_{\vec{k}+\vec{q}} - i\eta} \right] \tag{42a}$$

and

$$\Pi^{\rm HF}_{+-}(Q) = \int \frac{{\rm d}\vec{k}}{(2\pi)^3} \left[\frac{\theta(|\vec{k}+\vec{q}| - k_F^+)\theta(k_F^- - k)}{\omega + \omega^-_{\vec{k}} - \omega^+_{\vec{k}+\vec{q}} + i\eta} - \frac{\theta(k_F^+ - |\vec{k}+\vec{q}|)\theta(k - k_F^-)}{\omega + \omega^-_{\vec{k}} - \omega^+_{\vec{k}+\vec{q}} - i\eta} \right]. \tag{42b}$$

From the above formulas, the response region of the infinite, homogeneous neutron's system in the (ω, q) plane to a spin-flipping probe $(\sigma_\pm)$ is deduced by searching for the region where, e. g., $\Pi^{\rm HF}_{-+}(Q)$ develops an imaginary part. For this purpose we write

$$\mathrm{Im}\Pi^{\rm HF}_{-+}(Q) = \mathrm{Im}\Pi^{a}_{-+}(Q) + \mathrm{Im}\Pi^{b}_{-+}(Q), \tag{43}$$

being

$$\mathrm{Im}\Pi^{a}_{-+}(Q) = \int \frac{{\rm d}\vec{k}}{(2\pi)^3} \theta(|\vec{k}+\vec{q}| - k_F^-)\theta(k_F^+ - k)(-\pi)\delta(\omega + \omega^+_{\vec{k}} - \omega^-_{\vec{k}+\vec{q}}) \tag{44a}$$

and

$$\mathrm{Im}\Pi^{b}_{-+}(Q) = \int \frac{{\rm d}\vec{k}}{(2\pi)^3} \theta(k_F^- - |\vec{k}+\vec{q}|)\theta(k - k_F^+)(-\pi)\delta(\omega + \omega^+_{\vec{k}} - \omega^-_{\vec{k}+\vec{q}}). \tag{44b}$$

Hence, the first contribution to the imaginary part of $\Pi^{\rm HF}_{-+}$ (namely $\mathrm{Im}\Pi^{a}_{-+}(Q)$) lives in the domain

$$\frac{q^2}{2m} - \frac{k_F^+ q}{m} + \Delta\omega < \omega < \frac{q^2}{2m} + \frac{k_F^+ q}{m} + \Delta\omega, \tag{45a}$$

while the second one (namely $\mathrm{Im}\Pi^{b}_{+}(Q)$) lives in the domain

$$-\frac{q^2}{2m} - \frac{k_F^- q}{m} + \Delta\omega < \omega < -\frac{q^2}{2m} + \frac{k_F^- q}{m} + \Delta\omega. \tag{45b}$$

In the above we have set

$$\Delta\omega = -\frac{V_1}{2\pi^2}\left[(k_F^+)^3 - (k_F^-)^3\right] \tag{46}$$

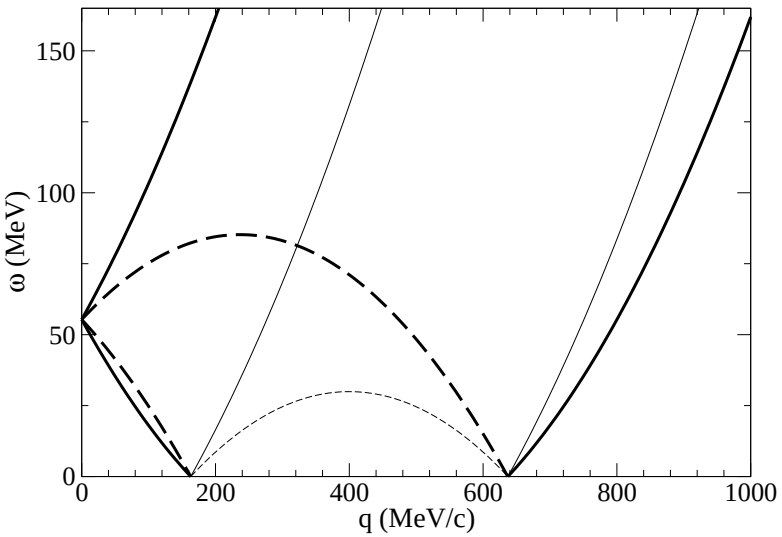

Fig. 9. The response region associated to $\Pi^{\rm HF}_{-+}$ (heavy lines) and to $\Pi^{\rm HF}_{+-}$ (light lines). The solid and dashed lines correspond to the first and second term in which we have split the imaginary part of $\Pi^{\rm HF}$, respectively (see Eq. (43)). The values for k_F^+ and k_F^- are the same as in Fig. 2.

and in our derivation we have exploited Eq. (6) and the relation

$$\omega^+_{\vec{k}} - \omega^-_{\vec{k}+\vec{q}} = \omega_{\vec{k}} - \omega_{\vec{k}+\vec{q}} - \Delta\omega = \omega_{\vec{k}} - \omega_{\vec{k}+\vec{q}} - \frac{1}{2m}((k_F^+)^2 - (k_F^-)^2), \qquad (47)$$

the last equality being valid for $V_{1,c}^{\rm lower} \leq V_1 \leq V_{1,c}^{\rm upper}$. For definitiveness, in the following we shall always choose $k_F^+ \geq k_F^-$,which implies $\Delta\omega \geq 0$.

The response region of $\Pi^{\rm HF}_{+-}(Q)$ can be derived along the same lines, yielding, instead of Eq. (45), the following expressions:

$$\frac{q^2}{2m} - \frac{k_F^- q}{m} - \Delta\omega < \omega < \frac{q^2}{2m} + \frac{k_F^- q}{m} - \Delta\omega \qquad (48a)$$

$$-\frac{q^2}{2m} - \frac{k_F^- q}{m} - \Delta\omega < \omega < -\frac{q^2}{2m} + \frac{k_F^- q}{m} - \Delta\omega. \qquad (48b)$$

It is of importance to observe that the response region related to $\Pi^{\rm HF}_{-+}$ ($\Pi^{\rm HF}_{+-}$) is shifted with respect to the symmetric case upward (downward) by an amount $\Delta\omega$ that directly reflects the size of the spontaneous breaking of the vacuum. The response regions for $\Pi^{\rm HF}_{-+}$ and $\Pi^{\rm HF}_{+-}$ are displayed in Fig. 9.

Concerning the response function, it is remarkable that the following symmetry relation holds valid: $\Pi^{\rm HF}_{-+}(\vec{q},\omega) = \Pi^{\rm HF}_{+-}(\vec{q},-\omega)$, as one can see by comparing Eqs. (42a) and (42b). Furthermore, note that, at variance with the symmetric vacuum case, now, for $\omega > 0$, also the second piece on the right hand side of Eqs. (42a) and (42b) contributes to the system's response, the more so, the

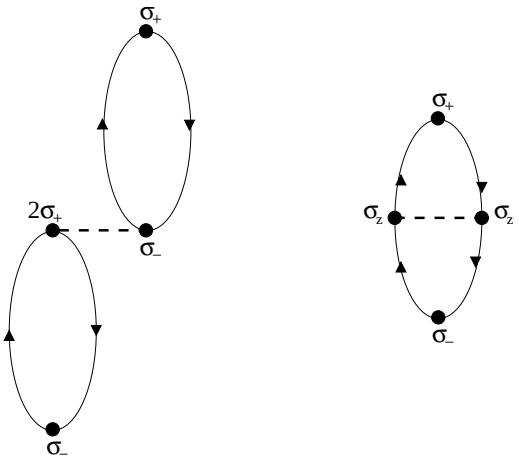

Fig. 10. The first order direct and exchange terms for $\Pi^{\rm RPA}_{-+}(Q)$.

smaller q is. To complete our analysis we quote in Appendix B the real and the imaginary part of $\Pi^{\rm HF}_{-+}$ and $\Pi^{\rm HF}_{+-}$.

It should finally be stated that similar results have been obtained in the context of asymmetric nuclear matter [18,19].

We turn now to discuss the RPA equations for Π_{-+} and Π_{+-}. The basic ingredients required for their deduction are the *first order* direct and exchange diagrams displayed (for Π_{+}) in Fig. 10. In our case of a zero-range interaction one finds

$$\Pi^{(1){\rm dir}}_{\mp\pm}(Q) = 2V_1\Pi^{\rm HF}_{\mp\pm}(Q)\Pi^{\rm HF}_{\mp\pm}(Q) \tag{49}$$

for the direct term and

$$\Pi^{(1){\rm ex}}_{\mp\pm}(Q) = V_1\Pi^{\rm HF}_{\mp\pm}(Q)\Pi^{\rm HF}_{\mp\pm}(Q) \tag{50}$$

for the exchange diagram. Hence the RPA series (which accounts for both contributions) can be easily resummed, leading to

$$\Pi^{\text{RPA-HF}}_{\mp\pm}(Q) = \frac{\Pi^{\rm HF}_{\mp\pm}(Q)}{1 - 3V_1\Pi^{\rm HF}_{\mp\pm}(Q)}. \tag{51}$$

To find the dispersion relation of the Goldstone bosons we search for the poles (if any) of the expression

$$\Pi^{\text{RPA-HF}}_{xx}(\vec{q},\omega) = \frac{\Pi^{\rm HF}_{-+}(\vec{q},\omega) + \Pi^{\rm HF}_{+-}(\vec{q},\omega) - 6V_1\Pi^{\rm HF}_{-+}(\vec{q},\omega)\Pi^{\rm HF}_{+-}(\vec{q},\omega)}{[1 - 3V_1\Pi^{\rm HF}_{-+}(\vec{q},\omega)][1 - 3V_1\Pi^{\rm HF}_{+-}(\vec{q},\omega)]} \tag{52}$$

for positive real ω.
From the numerical analysis we have found that of the two factors appearing in the denominator of Eq. (52) only the first one (since $k^+_F > k^-_F$) vanishes for just one real and positive value of ω at a given q. In Fig. 11 we display the

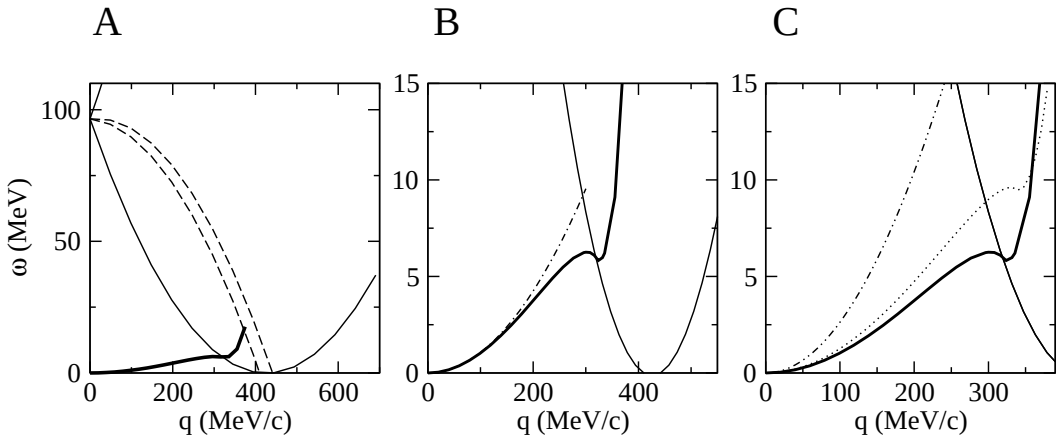

Fig. 11. The dispersion relation of the Goldstone boson for $k_F^+ = 426.01$ MeV/c (heavy solid lines), which corresponds to $V_1 = -189.25$ MeV fm^3. Also displayed are the response regions: the light solid and dashed lines correspond to Eqs. (45a) and (45b), respectively. In panel A one can appreciate how tiny the energy of the Goldstone boson is; in panel B, which enlarges panel A, one can assess the domain of validity of the parabolic dispersion relation of the Goldstone mode (dot-dashed line); in panel C the Goldstone mode is displayed for three different values of the interaction strength, namely $V_1 = -189.25$ (solid), -200 (dot) and -300 MeV fm^3 (dot-dot-dash).

solution of the equation

$$[1 - 3V_1 \mathrm{Re}\Pi^{\mathrm{HF}}_{-+}(\vec{q},\omega)] = 0, \tag{53}$$

which we expect to yield the dispersion relation of the Goldstone boson, should the RPA be a trustworthy theory for our many-body system. This turns out indeed to be the case, since for small q and ω the solution of Eq. (53) can be analytically expressed through the expansion of $\mathrm{Re}\Pi^{\mathrm{HF}}_{-+}(\vec{q},\omega)$, which reads

$$\lim_{q\to 0} \mathrm{Re}\Pi^{\mathrm{HF}}_{-+}(\vec{q},\omega) = \frac{mk_F^+}{4\pi^2}\frac{1}{\nu-\Delta\nu}\left[\frac{2}{3}(1-\xi^3) + \frac{1}{3}\frac{Q^2}{\nu-\Delta\nu}(1+\xi^3) + \frac{2}{15}\frac{Q^2}{(\nu-\Delta\nu)^2}(1-\xi^5)\right], \tag{54}$$

where

$$Q = \frac{q}{k_F^+},\ \xi = \frac{k_F^-}{k_F^+},\ \nu = \frac{m\omega}{(k_F^+)^2} \ \text{ and } \ \Delta\nu = \frac{-mV_1}{2\pi^2(k_F^+)^2}[(k_F^+)^3 - (k_F^-)^3].$$

From the above one gets the following dispersion relation, valid for small values of q:

$$\omega = \frac{q^2}{2m^\star} \tag{55}$$

with

$$m^\star = \frac{5(1+\xi)(1+\xi+\xi^2)}{(1-\xi)(1+3\xi+\xi^2)} m. \tag{56}$$

From Fig. 11 (panels B and C) it appears that the expression (55) actually remains valid over a substantial range of momenta. Thus, the solution of Eq. (53) truly corresponds to a type II Goldstone boson as it should. Microscopically this mode behaves like a particle-hole excitation (the particle being quite heavy). Physically it can be viewed as a twisting of the local spin orientation as the collective wave passes through the system [20].

Furthermore, and remarkably, it turns out that for $V_1 > V_{1,c}^{\rm upper}$ the Goldstone mode continues to exist with a dispersion relation that is parabolic over a range of momenta becoming larger as V_1 increases. For $V_{1,c}^{\rm lower} \leq V_1 \leq V_{1,c}^{\rm upper}$ the Goldstone mode displays instead an anomalous behavior: in fact, in this range of couplings, in correspondence to a specific momentum, the collective mode is characterized by a vanishing group velocity.

It is worth comparing the dispersion relation (55) with the formula for the energy levels of a rotational band. They are identical providing one replaces the momentum with the quantized angular momentum (of course, both quantities should not be too large) and the mass with the moment of inertia. From Fig. 11 (panel A) it is clearly apparent how tiny the energy of the Goldstone boson is, just as it happens for the rotational bands in nuclear and molecular physics.

In concluding this Section we display in Figs. 12, 13 and 14 the continuum response of the system to an x-aligned probe for the same momenta and vacua of Figs. 4, 5 and 6, where the response to a z-aligned probe was considered. We notice that

i) for a symmetric vacuum the energy-weighted sum rule is patently obeyed;
ii) the more the vacuum is broken, the more depleted the particle-hole continuum is;
iii) in accord with ii) the more the vacuum is broken, the stronger the Goldstone boson becomes. This item will be quantitatively addressed in the next section in the sum rule framework.

5 The moments of the response function

In this Section we investigate the non-energy-weighted (S_0) and the energy-weighted (S_1) sum rules, exploring their behavior when spontaneous symmetry breaking occurs in the vacuum.

Concerning S_1, it is well-known [21] that it is given by the following expression

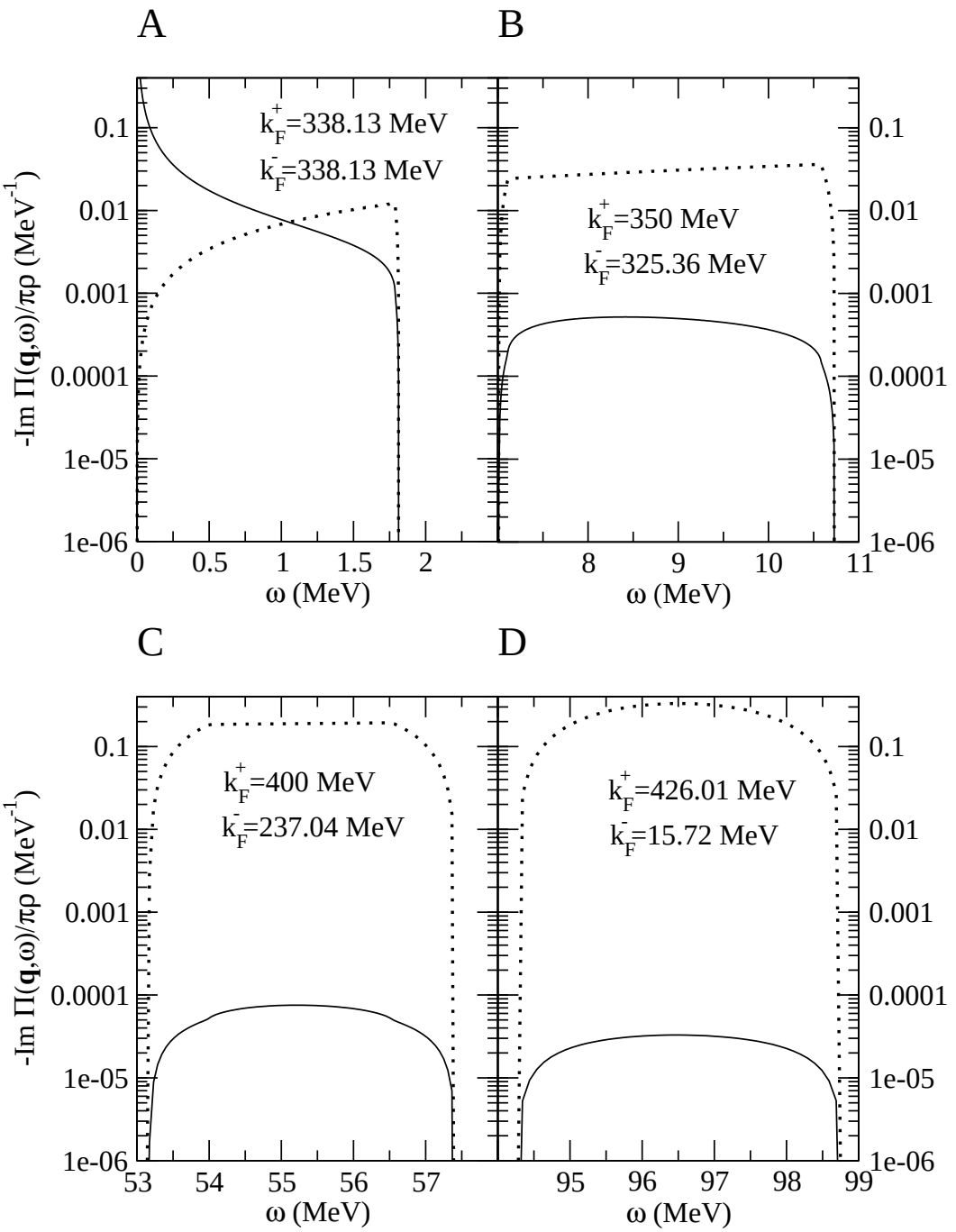

Fig. 12. The response of an infinite neutron's system to a x-aligned probe for $q = 5$ MeV/c. Panel (A) refers to the case of a symmetric vacuum ($k_F = k_F^+ = k_F^-$), panels (B) and (C) to a partially aligned broken vacuum, panel (D) to a totally broken, fully aligned vacuum. Dotted line: HF response, solid line: RPA-HF.

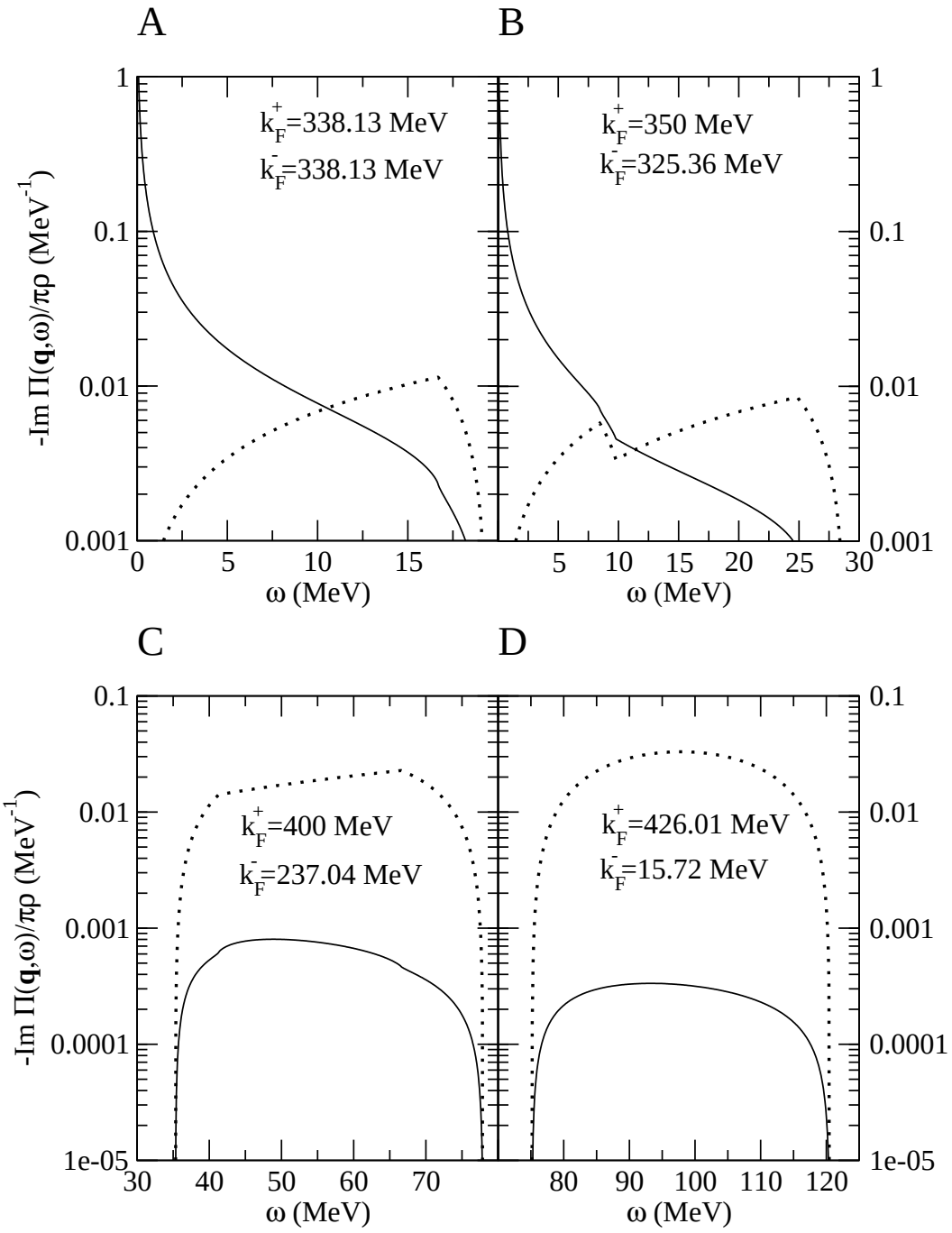

Fig. 13. The same as in Fig. 12 but for $q = 50$ MeV/c.

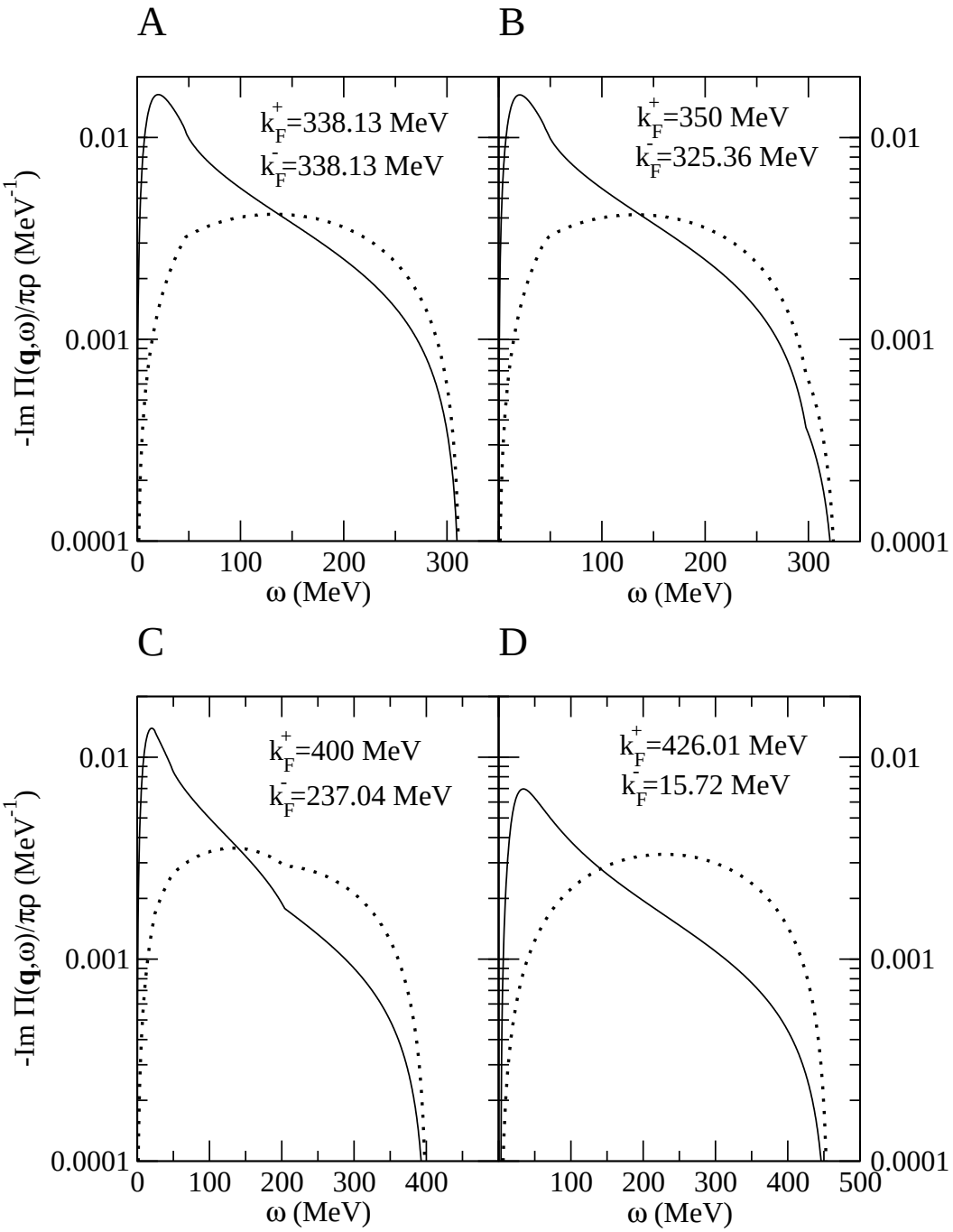

Fig. 14. As in Fig. 12 but for $q = 500$ MeV/c.

$$S_1(q) = \int_0^\infty \mathrm{d}\omega\, \omega \frac{-\mathrm{Im}\Pi(\vec{q},\omega)}{\pi\rho} = \frac{1}{2}\langle 0|[\widehat{O},[\hat{H},\widehat{O}]]|0\rangle. \tag{57}$$

For the density response of a non-interacting gas of fermions of mass m the above is indeed fulfilled and yields

$$S_1^{\mathrm{free}}(q) = \int_0^\infty \mathrm{d}\omega\, \omega \frac{-\mathrm{Im}\Pi^0(\vec{q},\omega)}{\pi\rho} = \frac{q^2}{2m}. \tag{58}$$

In general, however, Eq. (57) is violated by most of the many-body frameworks, the remarkable exception being the RPA-HF theory. In fact, the Thouless theorem [22] states that if the system's response is computed in RPA-HF and the expectation value on the right hand side of Eq. (57) is taken in the HF ground state, then the sum rule is fulfilled. We have indeed verified it by computing numerically with very good accuracy the left hand side of Eq. (57) and by working out the HF expectation value of the double commutator in the same equation — which of course yields $q^2/2m$, if one employs the interaction (19) and the vertex (18).

Remarkably, even when the vacuum is broken S_1 keeps the above value, as it can be inferred from the results reported in Tables 1, 2 and 3. Note that this outcome could also be proved along the lines followed in Ref. [23] in the case of a symmetric vacuum. Conceptually, it relates to the very meaning of S_1, namely of expressing the particle number conservation (or the global gauge invariance) of the theoretical framework and in the non-symmetric vacuum it is the rotational — and not the gauge — invariance to be broken.

In this instance, at variance with the situation where the probe acts in the direction of the spontaneous magnetization, when the spin-flipping probe is directed orthogonally to the latter, S_1 is contributed to not only by the particle-hole continuum, but by the collective Goldstone mode as well. Indeed, from Eq. (51) one has

$$\mathrm{Im}\Pi_{-+}^{\text{RPA-HF}}(Q) = \frac{\mathrm{Im}\Pi_{-+}^{\mathrm{HF}}(Q)}{\left[1 - 3V_1 \mathrm{Re}\Pi_{-+}^{\mathrm{HF}}(Q)\right]^2 + 9V_1^2\left[\mathrm{Im}\Pi_{-+}^{\mathrm{HF}}(Q)\right]^2}, \tag{59}$$

which, in the region where $\mathrm{Im}\Pi_{-+}^{\mathrm{HF}}(Q)$ vanishes, yields

$$\begin{aligned}\mathrm{Im}\Pi_{-+}^{\text{RPA-HF}}(Q) &= \pi \mathrm{Re}\Pi_{-+}^{\mathrm{HF}}(Q)\delta[1 - 3V_1\mathrm{Re}\Pi_{-+}^{\mathrm{HF}}(Q)] \\ &= \frac{\pi}{9V_1^2}\frac{1}{\left|\dfrac{\partial \mathrm{Re}\Pi_{-+}^{\mathrm{HF}}(Q)}{\partial\omega}\right|_{\omega=\omega_+(q)}}\delta[\omega - \omega_+(q)],\end{aligned} \tag{60}$$

with $\omega_+(q)$ the solution of Eq. (53), that is the Goldstone boson dispersion relation.

k_F^+	S_0^{HF}	$S_0^{\text{RPA-HF}}$	S_1^{HF}	$S_1^{\text{RPA-HF}}$	$\Delta\omega$
338.130028	0.0111	(0.0819+0)	0.013312	(0.013312+0)	0
350	0.1091	(0.00152+0.10754)	0.9795	(0.013295+0.000017)	8.860
400	0.65549	(0.000228+0.65527)	36.248	(0.012594+0.000718)	55.279
426.01	1.000	(0.000111+0.99979)	96.510	(0.010664+0.002686)	96.505

Table 1

The non-energy-weighted and energy-weighted sum rules at $q = 5$ MeV/c, corresponding to $q^2/2m = 0.0133120$ MeV. The Fermi momentum $k_F^+ = 338.130028$ MeV/c corresponds to a symmetric vacuum, whereas $k_F^+ = 426.01$ MeV/c corresponds to an almost completely broken vacuum (ground state fully aligned in spin space). In the columns associated with the RPA-HF theory, the first figure represents the contribution to S_0 and S_1, respectively, arising from the particle-hole continuum; the second figure the one arising from the collective Goldstone mode.

k_F^+	S_0^{HF}	$S_0^{\text{RPA-HF}}$	S_1^{HF}	$S_1^{\text{RPA-HF}}$	$\Delta\omega$
338.130028	0.1107	(0.5842+0)	1.33120	(1.33120+0)	0
350	0.1374	(0.5340+0)	2.29744	(1.33120+0)	8.860
400	0.6555	(0.0233+0.6322)	37.566	(1.26414+0.06706)	55.279
426.01	0.9999	(0.0111+0.9888)	97.827	(1.07098+0.26025)	96.505

Table 2

The same as in Table 1 but for $q = 50$ MeV/c, corresponding to $q^2/2m = 1.33120$ MeV.

k_F^+	S_0^{HF}	$S_0^{\text{RPA-HF}}$	S_1^{HF}	$S_1^{\text{RPA-HF}}$	$\Delta\omega$
338.130028	0.907	1.528	133.120	133.120	0
350	0.908	1.524	134.087	133.120	8.860
400	0.951	1.359	169.356	133.120	55.279
426.01	1.000	1.000	229.616	133.120	96.505

Table 3

The same as in Table 1 but for $q = 500$ MeV/c, corresponding to $q^2/2m = 133.120$ MeV.

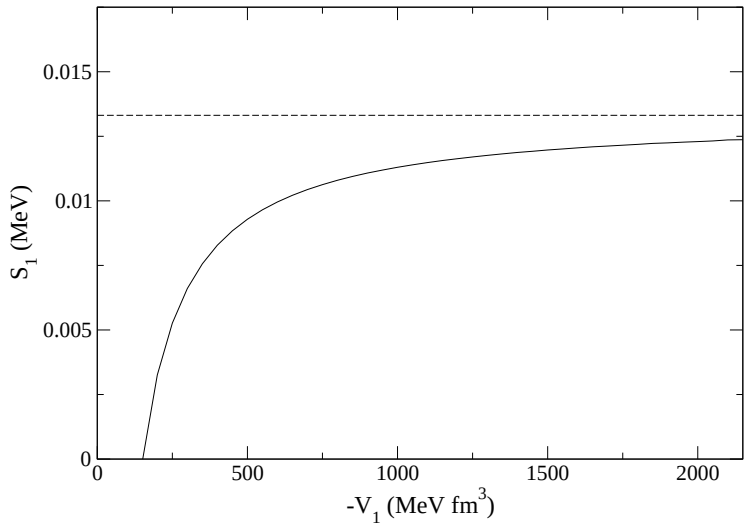

Fig. 15. Contribution of the Goldstone mode to the energy-weighted sum rule as a function of the interaction strength for $q = 5$ MeV/c (solid line); the curve starts at $V_{1,c}^{\rm lower} = -159.16$ MeV fm^3. The dashed line represents the saturation value $q^2/2m = 0.0133120$ MeV.

Actually, this contribution grows with the amount of symmetry breaking in the vacuum, which, in turn, grows with the strength of the force V_1. For $V_1 = V_{1,c}^{\rm upper}$, namely when the vacuum is fully aligned in spin-space, the Goldstone mode accounts for roughly 25% of the energy-weighted sum rule, as it can be deduced from the figures reported in Tables 1 and 2. For still larger values of V_1, this amounts keeps increasing until, for $V_1 \to \infty$, it exhausts the sum rule, as it is seen in Fig. 15, where the Goldstone mode contribution to S_1 is displayed versus V_1. Of course, for large values of q the Goldstone boson no longer exists (Table 3).

Concerning the non-energy-weighted sum rule in a symmetric vacuum and for a non-interacting system of fermions one has the well-known result

$$\begin{aligned} S_0(q) &= \frac{3}{4}\frac{q}{k_F}\left[1 - \frac{1}{12}\left(\frac{q}{k_F}\right)^2\right] \qquad && q \le 2k_F \\ &= 1 && q > 2k_F, \end{aligned} \tag{61}$$

which is conserved in the HF theory, but not in RPA or RPA-HF. When the vacuum is spontaneously broken by our ferromagnetic force, one finds that the impact of the Pauli correlations on S_0 is lowered with respect to the symmetric vacuum case and decreases as the amount of the symmetry breaking grows, as it is apparent from Tables 1, 2 and 3. In particular, for a fully broken vacuum, S_0 is just 1 for any q — that is the value occurring in the symmetric vacuum for $q \ge 2k_F$ — both when our system is explored in the longitudinal or in

the transverse direction by a spin-dependent probe: the system's constituents no longer feel the Pauli principle, as it should be expected since in the fully magnetized case only one species of particles is present.

The reduced influence of the Pauli principle, when the system in only partially aligned, with respect to the situation occurring in the symmetric vacuum, can be exploited to investigate (using a spin-flipping probe) how the collectivity of the Goldstone mode is affected by the degree of spontaneous symmetry breaking of the vacuum. In fact, in Tables 1 and 2 one sees that the less effective the Pauli correlations are, the more collective the Goldstone boson is.

6 Conclusions

In the present study we have dealt with an infinite, non-relativistic, homogeneous system of neutrons interacting through a simple ferromagnetic force of Heisenberg type, our aim being to discuss general aspects of the spontaneous symmetry breaking associated with a quantum phase transition. Although this theme has been much addressed in the past for generic spin 1/2 fermions (see, e. g., Ref. [8]), still we felt it useful to analyze in more detail the dependence upon the interaction range of the critical values of the coupling and the excitation spectrum of a system undergoing a quantum phase transition.

Concerning the latter, we like to remind that the symmetry breaking taking place in our system, namely the onset of a permanent, spontaneous magnetization, stems from a well identified physical source, a situation very different, for example, from the electroweak symmetry breaking in the standard model, where the responsible for such an occurrence, namely the Higgs boson, is still searched for three decades after having been conjectured. Indeed, in our system — just like in a ferromagnet the electromagnetic interaction between neighboring atoms lines up their spins parallel to each other — the force between neighboring neutrons produces the same effect, provided that the strength of the interaction exceeds some critical value, $V_{1,c}^{\rm lower}$. How close the neutrons should be for the phase transition to occur or, equivalently, how the range of the interaction affects the value of $V_{1,c}^{\rm lower}$? We have answered this question both numerically and analytically, finding out, as expected, that the longer the range, the weaker the strength of the coupling should be in order to induce the spontaneous breaking of a symmetry. A further natural question to ask is how large V_1 should be for the system to become fully magnetized. Also for this problem we provide a numerical and an analytic answer, again confirming the above referred to correlation between strength and range.

We have next analyzed the spectrum of the system (or, equivalently, the re-

sponse functions to external probes acting on the spin of the constituents), following its evolution with the amount of spontaneous symmetry breaking occurring in the ground state. Probing the system along the direction of the spontaneous magnetization, the chief feature of the response function relates to the occurrence of two distinct peaks, which reflect both the action of the ferromagnetic force and of the Pauli principle. Indeed, the two peaks merge at large transferred momenta, where the latter disappears.

In the direction orthogonal to the magnetization, on the other hand, a collective Goldstone mode shows up as required by the theory. Its dispersion relation is indeed parabolic, as it should, over a momentum range that increases as the coupling strength V_1 increases. Actually, for $V_1 \to \infty$, the Goldstone boson exhausts the energy-weighted sum rule and its dispersion relation becomes a perfect parabola. Notably, for a strength V_1 intermediate between the two critical values $V_{1,c}^{\rm lower}$ and $V_{1,c}^{\rm upper}$, the Goldstone boson dispersion relation displays an anomalous non-parabolic behavior, entailing the existence of a wavelength associated with a vanishing group velocity of the collective mode. We conjecture this to be a distinctive signature of the Goldstone boson in the non-relativistic regime.

In spite of the simplicity of our interaction, which has of course no pretense of being realistic, it appears that our research bears significance for the physics of the neutron stars, since it explores the extension of the many-body response theory to the situation associated with a broken vacuum in a spin space, which is required for the assessment of the magnetic field that neutron stars host. A lot of work has actually been lately done on this issue: interestingly, it appears that simple effective interactions — such as the Skyrme ones — give indeed rise to a phase transition of second kind [2,3], whereas more microscopic many-body approaches — such as the Brueckner-Hartree-Fock formalism [4] or quantum simulations [5,6] — give no indication of a quantum phase transition. Generally speaking, this striking difference can be related to the different predictions these models give for the particle-hole spin interaction at neutron star densities: attractive in the Skyrme models and repulsive in calculations based on realistic nucleon-nucleon potentials [24]. Unfortunately, at present there are no direct phenomenological constraints on this component of the effective nuclear interaction at densities relevant for the neutron stars.

In connection with the possible application of the concept of spontaneous symmetry breaking to the physics of the atomic nuclei, it should be of course realized that in finite systems the notion of phase transition applies only approximately. Yet, one is naturally lead to think of heavy nuclei, where the isospin symmetry is broken, leading to ground state configurations quite similar to the ones we have been considering in the spin space. However, in isospace the symmetry is broken explicitly (by the Coulomb force) and not spontaneously (as in our case). Thus, although for heavy nuclei the response region of the

system in the (ω, q) plane turns out to be very similar in both cases [18], in nuclear matter no collective Goldstone boson should show up in the small ω, small q corner of the (ω, q) plane. Furthermore, in the isospin particle-hole channel — the one appropriate to the present considerations — no attraction seems to exist.

Appendices

A Probing the system in the symmetric direction: the RPA matrix elements

Here we derive the exact expression for $\Pi_{zz}^{\mathrm{RPA,b}}$. In Eq. (26) we made an ansatz on the form of the equation obeyed by the latter. We have now to fix the matrix elements of the potential entering into Eq. (27). This can be easily done expanding Eq. (26) to first order in V_1 and then matching the result obtained in this way with the explicit expression coming from the evaluation of the first order diagrams in Figs. (A.1) and (A.2). From Eq. (26) it follows immediately that

$$\widehat{\Pi} = (1 - \widehat{\Pi}^0 \widehat{V})^{-1} \widehat{\Pi}^0. \tag{A.1}$$

Hence the evaluation of $\widehat{\Pi}$ simply amounts to invert a 2×2 matrix. We get:

$$\widehat{\Pi} = \frac{1}{D} \begin{pmatrix} \Pi^0_{++}(1 - \Pi^0_{--} V_d) & \Pi^0_{++} V_{od} \Pi^0_{--} \\ \Pi^0_{++} V_{od} \Pi^0_{--} & \Pi^0_{--}(1 - \Pi^0_{++} V_d) \end{pmatrix}, \tag{A.2}$$

where

$$D = 1 - V_d(\Pi^0_{++} + \Pi^0_{--}) + \Pi^0_{++}\Pi^0_{--}(V_d^2 - V_{od}^2). \tag{A.3}$$

The complete RPA result is thus given by

$$\begin{aligned} \Pi^{\mathrm{RPA}} &= \Pi_{++} + \Pi_{--} + 2\Pi_{+-} \\ &= \frac{1}{D}\left[\Pi^0_{++} + \Pi^0_{--} + 2\Pi^0_{++}\Pi^0_{--}(V_{od} - V_d)\right], \end{aligned} \tag{A.4}$$

which can be expanded to first order in V obtaining

$$\Pi_{zz}^{(1)\mathrm{RPA}} = \Pi^0_{++} + \Pi^0_{--} + \Pi^0_{++} V_d \Pi^0_{++} + \Pi^0_{--} V_d \Pi^0_{--} + 2\Pi^0_{++} V_{od} \Pi^0_{--}. \tag{A.5}$$

The direct contribution to $\Pi_{zz}^{(1)\mathrm{RPA}}$ comes from the diagram in Fig. A.1 and reads

$$\Pi_{zz}^{(1)\mathrm{dir}} = \Pi^0_{++} V_1 \Pi^0_{++} + \Pi^0_{--} V_1 \Pi^0_{--} + 2\Pi^0_{++} V_{od} \Pi^0_{--}. \tag{A.6}$$

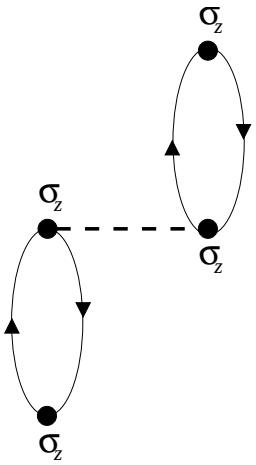

Fig. A.1. The first order direct term contributing to $\Pi_{zz}^{\rm RPA}$.

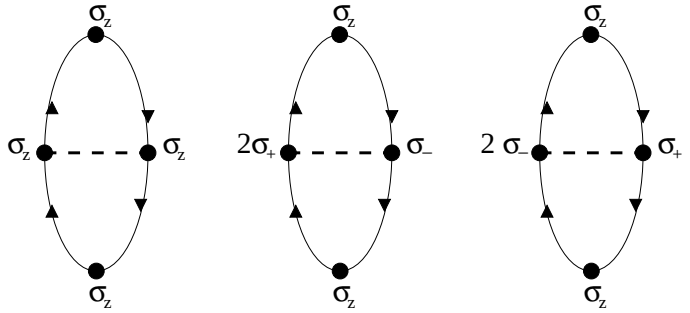

Fig. A.2. The first order exchange terms contributing to $\Pi_{zz}^{\rm RPA}$.

The first order exchange contribution comes from the three diagrams in Fig. A.2 and reads

$$\Pi_{zz}^{(1)\rm ex} = -\Pi^0_{++}V_1\Pi^0_{++} - \Pi^0_{--}V_1\Pi^0_{--} + 4\Pi^0_{++}V_{od}\Pi^0_{--}. \tag{A.7}$$

If one chooses to keep only the direct contribution to the first order result for $\widehat{\Pi}$ (*ring approximation*) then, from the matching with Eq. (A.5), it follows that

$$V_d^{\rm dir} = V_1,\ V_{od}^{\rm dir} = V_1 \ \Rightarrow \quad \widehat{V}^{\rm dir} = \begin{pmatrix} V_1 & V_1 \\ V_1 & V_1 \end{pmatrix}. \tag{A.8}$$

On the other hand, keeping only the first order exchange contribution, the matching with Eq. (A.5) allows one to resum the *ladder series* obtaining

$$V_d^{\rm ex} = -V_1,\ V_{od}^{\rm ex} = 2V_1 \ \Rightarrow \quad \widehat{V}^{\rm ex} = \begin{pmatrix} -V_1 & 2V_1 \\ 2V_1 & -V_1 \end{pmatrix}. \tag{A.9}$$

Finally, from the matching of Eq. (A.5) with all the four diagrams in Figs. (A.1) and (A.2), one gets the *full RPA result* (direct + exchange):

$$V_d^{\rm RPA}=0,\ V_{od}^{\rm RPA}=3V_1\ \Rightarrow\quad \widehat{V}^{\rm RPA}=\begin{pmatrix}0 & 3V_1\\ 3V_1 & 0\end{pmatrix}. \tag{A.10}$$

B The HF polarization propagator in a broken vacuum

In this appendix we display how the calculations leading to $\Pi^{\rm HF}_{\mp\pm}$ (which enter into Eq. (51) for $\Pi^{\rm RPA}_{\mp\pm}$) can be performed analytically in a quite straightforward way following a procedure first introduced in Ref. [25]. Starting from the expression for $\Pi^{\rm HF}_{-+}$ given in Eq. (42a), one introduces the *particle-hole propagator* in the HF approximation, defined as:

$$G^{\rm HF}_{\rm ph}(\vec{k},\vec{q},\omega)=\frac{\theta(|\vec{k}+\vec{q}|-k_F^-)\theta(k_F^+-k)}{\omega+\omega^+_{\vec{k}}-\omega^-_{\vec{k}+\vec{q}}+i\eta}-\frac{\theta(k_F^--|\vec{k}+\vec{q}|)\theta(k-k_F^+)}{\omega+\omega^+_{\vec{k}}-\omega^-_{\vec{k}+\vec{q}}-i\eta}. \tag{B.1}$$

The above expression can be manipulated in the following way:

$$\begin{aligned}G^{\rm HF}_{\rm ph}(\vec{k},\vec{q},\omega)=&\frac{\theta(|\vec{k}+\vec{q}|-k_F^-)\theta(k_F^+-k)}{\omega+\omega^+_{\vec{k}}-\omega^-_{\vec{k}+\vec{q}}+i\eta}+\frac{\theta(k_F^--|\vec{k}+\vec{q}|)\theta(k-k_F^+)}{-\omega-\omega^+_{\vec{k}}+\omega^-_{\vec{k}+\vec{q}}+i\eta}\\ &+\frac{\theta(k_F^--|\vec{k}+\vec{q}|)\theta(k_F^+-k)}{\omega+\omega^+_{\vec{k}}-\omega^-_{\vec{k}+\vec{q}}+i\eta_\omega}+\frac{\theta(k_F^--|\vec{k}+\vec{q}|)\theta(k_F^+-k)}{-\omega-\omega^+_{\vec{k}}+\omega^-_{\vec{k}+\vec{q}}-i\eta_\omega}\\ =&\frac{\theta(k_F^+-k)-\theta(k_F^--|\vec{k}+\vec{q}|)}{\omega-\omega^-_{\vec{k}+\vec{q}}+\omega^+_{\vec{k}}+i\eta_\omega},\end{aligned} \tag{B.2}$$

being $\eta_\omega=\mathrm{sign}(\omega)\eta$. Hence, expressing $\Pi^{\rm HF}_{-+}$ in terms of the particle-hole propagator

$$\Pi^{\rm HF}_{-+}(q,\omega)=\int\frac{\mathrm{d}\vec{k}}{(2\pi)^3}G^{\rm HF}_{\rm ph}(\vec{k},\vec{q},\omega)=\int\frac{\mathrm{d}\vec{k}}{(2\pi)^3}\frac{\theta(k_F^+-k)-\theta(k_F^--|\vec{k}+\vec{q}|)}{\omega-\omega^-_{\vec{k}+\vec{q}}+\omega^+_{\vec{k}}+i\eta_\omega}, \tag{B.3}$$

and performing the change of variable $\vec{k}+\vec{q}\to\vec{k}$ within the integral for the second contribution, one gets:

$$\Pi^{\rm HF}_{-+}(q,\omega)=\int\frac{\mathrm{d}\vec{k}}{(2\pi)^3}\left[\frac{\theta(k_F^+-k)}{\omega-\omega^-_{\vec{k}+\vec{q}}+\omega^+_{\vec{k}}+i\eta_\omega}-\frac{\theta(k_F^--k)}{\omega+\omega^+_{\vec{k}+\vec{q}}-\omega^-_{\vec{k}}+i\eta_\omega}\right]. \tag{B.4}$$

The energy denominators in the equation above can be written as

$$\omega - \omega^-_{\vec{k}+\vec{q}} + \omega^+_{\vec{k}} = \omega - \frac{q^2}{2m} - \frac{\vec{q}\cdot\vec{k}}{m} - \Delta\omega \tag{B.5a}$$

$$\omega + \omega^+_{\vec{k}+\vec{q}} - \omega^-_{\vec{k}} = \omega + \frac{q^2}{2m} + \frac{\vec{q}\cdot\vec{k}}{m} - \Delta\omega, \tag{B.5b}$$

where

$$\Delta\omega = -\frac{V_1}{2\pi^2}\left[(k_F^+)^3 - (k_F^-)^3\right]. \tag{B.6}$$

Note that at equilibrium V_1 is related to $k_F^\pm$ through Eq. (6) and one gets to the expression (46) of Section 4.

It is particularly convenient to introduce the *scaling variables*:

$$\psi_\pm = \frac{1}{k_F^\pm}\left(\frac{m\omega}{q} - \frac{q}{2}\right) \tag{B.7a}$$

$$\Delta\psi_\pm = \frac{m\Delta\omega}{k_F^\pm q}. \tag{B.7b}$$

In terms of the above variables we can write:

$$\omega - \omega^-_{\vec{k}+\vec{q}} + \omega^+_{\vec{k}} = \frac{k_F^- q}{m}\left(\psi_- - \Delta\psi_- - \frac{\hat{q}\cdot\vec{k}}{k_F^-}\right) \tag{B.8a}$$

$$\omega + \omega^+_{\vec{k}+\vec{q}} - \omega^-_{\vec{k}} = \frac{k_F^+ q}{m}\left(\psi_+ - \Delta\psi_+ + \frac{q}{k_F^+} + \frac{\hat{q}\cdot\vec{k}}{k_F^+}\right). \tag{B.8b}$$

Hence $\Pi^{\rm HF}_{-+}$ can be expressed analytically as follows:

$$\Pi^{\rm HF}_{-+}(q,\omega) = \frac{m}{q}\frac{1}{(2\pi)^2}\left[(k_F^-)^2\mathcal{Q}^{(0)}(\psi_- - \Delta\psi_-) - (k_F^+)^2\mathcal{Q}^{(0)}(\psi_+ - \Delta\psi_+ + \bar{q}_+)\right], \tag{B.9}$$

being $\bar{q}_\pm = q/k_F^\pm$. Analogously, for $\Pi^{\rm HF}_{+-}$ one gets:

$$\Pi^{\rm HF}_{+-}(q,\omega) = \frac{m}{q}\frac{1}{(2\pi)^2}\left[(k_F^+)^2\mathcal{Q}^{(0)}(\psi_+ + \Delta\psi_+) - (k_F^-)^2\mathcal{Q}^{(0)}(\psi_- + \Delta\psi_- + \bar{q}_-)\right]. \tag{B.10}$$

The expressions reported above allow us to write $\mathrm{Re}\Pi^{\rm HF}_\mp$ ($\mathrm{Re}\Pi^{\rm HF}_\pm$) and $\mathrm{Im}\Pi^{\rm HF}_\mp$ ($\mathrm{Im}\Pi^{\rm HF}_\pm$) in terms of Legendre polynomials and functions of second kind, P_n and Q_n, respectively. Indeed it is easy to show that

$$\mathrm{Re}\mathcal{Q}^{(0)}(\psi) = \frac{2}{3}[Q_0(\psi) - Q_2(\psi)] \tag{B.11a}$$

$$\mathrm{Im}\mathcal{Q}^{(0)}(\psi) = -\mathrm{sign}(\omega)\theta(1-\psi^2)\frac{\pi}{3}[P_0(\psi) - P_2(\psi)]. \tag{B.11b}$$

References

[1] F. Iachello, in "From Nuclei and their Constituents to Stars", A. Molinari et al., eds., IOS, Amsterdam, 2003, p. 1.

[2] J. Rikovska Stone, J. C. Miller, R. Koncewicz, P. D. Stevenson and M. R. Strayer, *Phys. Rev. C* **68** (2003) 034324.

[3] A. A. Isayev and J. Yang, *Phys. Rev. C* **69** (2004) 025801.

[4] I. Vidaña, A. Polls and A. Ramos, *Phys. Rev. C* **65** (2002) 035804.

[5] S. Fantoni, A. Sarsa and K. E. Schmidt, *Phys. Rev. Lett.* **87** (2001) 181101.

[6] A. Sarsa, S. Fantoni, K. E. Schmidt and F. Pederiva, *Phys. Rev. C* **68** (2003) 024308.

[7] A. Beraudo, A. De Pace, M. Martini and A. Molinari, *Ann. Phys. (N.Y.)* **311** (2004) 81.

[8] K. Huang, "Quantum Field Theory: from Operators to Path Integrals", Wiley, New York, 1998, p. 294.

[9] A. Bohr and B. Mottelson, "Nuclear Structure Vol.II", Benjamin, Reading, 1975, p. 490.

[10] H. B. Nielsen and S. Chada, *Nucl. Phys. B* **105** (1976) 445.

[11] J. Cardy, "Scaling and Renormalization in Statistical Physics", Cambridge University Press, New York, 1996, p. 104.

[12] K. Huang, "Statistical Mechanics", Wiley, New York, 1987, p. 341.

[13] W. M. Alberico, R. Cenni, M. B. Johnson and A. Molinari, *Ann. Phys. (N.Y.)* **138** (1982) 178.

[14] A. L. Fetter and J. D. Walecka, "Quantum Theory of Many-Particle Systems", McGraw-Hill, New York, 1971, p. 158.

[15] W. M. Alberico, M. Ericson, A. Molinari and Z.X. Wang, *Phys. Lett. B* **223** (1989) 37.

[16] M. B. Barbaro, A. Molinari, F. Palumbo and M. R. Quaglia, *Phys. Rev. C* (in print).

[17] I. Low and A. V. Manohar, *Phys. Rev. Lett.* **88** (2002) 101602.

[18] W. M. Alberico, A. Drago and C. Villavecchia, *Nucl. Phys. A* **505** (1989) 309.

[19] K. Takayanagi and T. Cheon, *Phys. Lett. B* **294** (1992) 14.

[20] D. Forster, "Hydrodynamic, fluctuations, broken symmetry and correlation functions", Benjamin, Reading, 1975.

[21] P. Ring and P. Schuck, "The Nuclear Many-Body Problem", Springer-Verlag, Berlin, 1980, p. 331.

[22] D. J. Thouless, *Nucl. Phys.* **22** (1961) 78.

[23] K. Takayanagi, *Nucl. Phys. A* **510** (1990) 162.

[24] S. Reddy, M. Prakash, J. M. Lattimer and J. A. Pons, *Phys. Rev. C* **59** (1999) 2888.

[25] A. De Pace, *Nucl. Phys. A* **635** (1998) 163.